Eur. Phys. J. C (2018) 78:714
https://doi.org/10.1140/epjc/s10052-018-6174-5

THE EUROPEAN PHYSICAL JOURNAL C

Regular Article - Theoretical Physics

Two loop electroweak corrections to $\bar{B} \to X_s\gamma$ and $B_s^0 \to \mu^+\mu^-$ in the B-LSSM

Jin-Lei Yang[1,a], **Tai-Fu Feng**[1,b], **Shu-Min Zhao**[1], **Rong-Fei Zhu**[1], **Xiu-Yi Yang**[2], **Hai-Bin Zhang**[1,c]

[1] Department of Physics, Hebei University, Baoding 071002, China
[2] Department of Science, University of Science and Technology Liaoning, Anshan 114051, China

Received: 15 May 2018 / Accepted: 22 August 2018 / Published online: 5 September 2018

Abstract The rare decays $\bar{B} \to X_s\gamma$ and $B_s^0 \to \mu^+\mu^-$ are important to research new physics beyond the standard model (SM). In this work, we investigate two loop electroweak corrections to $\bar{B} \to X_s\gamma$ and $B_s^0 \to \mu^+\mu^-$ in the minimal supersymmetric extension of the SM with local $B-L$ gauge symmetry (B-LSSM), under a minimal flavor violating assumption for the soft breaking terms. In this framework, new particles and new definition of squarks can affect the theoretical predictions of these two processes, with respect to the MSSM. Considering the constraints from updated experimental data, the numerical results show that the B-LSSM can fit the experimental data for the branching ratios of $\bar{B} \to X_s\gamma$ and $B_s^0 \to \mu^+\mu^-$. The results of the rare decays also further constrain the parameter space of the B-LSSM.

1 Introduction

The study on B physics is one of the most promising windows to detect the new physics beyond the standard model (SM), since the theoretical evaluations on the relevant physical quantities are not seriously affected by the uncertainties due to the QCD effects. Recently, the average experimental data on the branching ratios of $\bar{B} \to X_s\gamma$ and $B_s^0 \to \mu^+\mu^-$ are shown as [1–4]

$$\begin{aligned} Br(\bar{B} \to X_s\gamma) &= (3.49 \pm 0.19) \times 10^{-4}, \\ Br(B_s^0 \to \mu^+\mu^-) &= (2.9^{+0.7}_{-0.6}) \times 10^{-9}. \end{aligned} \tag{1}$$

The SM predicts the $\bar{B} \to X_s\gamma$ and $B_s^0 \to \mu^+\mu^-$ branching ratios to be [5–13]

$$\begin{aligned} Br(\bar{B} \to X_s\gamma) &= (3.36 \pm 0.23) \times 10^{-4}, \\ Br(B_s^0 \to \mu^+\mu^-) &= (3.23 \pm 0.27) \times 10^{-9}, \end{aligned} \tag{2}$$

which are in agreement with the experimental results very well. So, the precise measurements on the rare B-decay processes constrain the new physics beyond SM strictly.

In extensions of the SM, the supersymmetry is considered as one of the most plausible candidates. Actually, the analyses of constraints on parameters in the minimal supersymmetric extension of the SM (MSSM) are discussed in detail [14–21]. The authors of Refs. [22–24] present the calculation of the rate inclusive decay $B \to X_s\gamma$ in the two-Higgs doublet model (THDM). The supersymmetric effect on $B \to X_s\gamma$ is discussed in Refs. [25–31] and the next-to-leading order (NLO) QCD corrections are given in Ref. [32]. The branching ratio for $B_s \to l^+l^-$ in THDM and supersymmetric extensions of the SM has been calculated in Refs. [33–38]. The hadronic B decays [39] and CP-violation in these processes [40] have also been discussed. The authors of Ref. [41] have discussed possibility of observing supersymmetric effects in rare decays $B \to X_s\gamma$ and $B \to X_s e^+e^-$ at the B-factory. The supersymmetric effects on these processes are very interesting and studies on them may shed some light on the general characteristics of the supersymmetric model. A relevant review can be found in Refs. [42,43].

The minimal supersymmetric extension of the SM with local $B-L$ gauge symmetry (B-LSSM) [44,45] is based on the gauge symmetry group $SU(3)_C \otimes SU(2)_L \otimes U(1)_Y \otimes U(1)_{B-L}$, where B stands for the baryon number and L stands for the lepton number respectively. Besides accounting elegantly for the existence and smallness of the left-handed neutrino masses, the B-LSSM also alleviates the little hierarchy problem of the MSSM [46], because the exotic singlet Higgs and right-handed (s)neutrinos [47–55] release additional parameter space from the LEP, Tevatron and LHC constraints. The invariance under $U(1)_{B-L}$ gauge group imposes the R-parity conservation which is assumed in the MSSM to avoid proton decay. And R-parity conservation can be maintained if $U(1)_{B-L}$ symmetry is broken spontaneously [56]. Furthermore, it could help to understand the origin of R-

[a] e-mail: JLYangJL@163.com
[b] e-mail: fengtf@hbu.edu.cn
[c] e-mail: hbzhang@hbu.edu.cn

parity and its possible spontaneous violation in the supersymmetric models [57–59] as well as the mechanism of leptogenesis [60,61]. Moreover, the model can provide much more candidates for the Dark Matter comparing that with the MSSM [62–65]. In this work, we analyze two loop electroweak corrections to $\bar{B} \to X_s\gamma$ and $B_s^0 \to \mu^+\mu^-$ in the B-LSSM, under a minimal flavor violating assumption for the soft breaking terms. In this framework, new couplings and particles make new contributions to both of these processes with respect to the MSSM. The numerical results of the rare decays also further constrain the parameter space of the model.

Our presentation is organized as follows. In Sect. 2, the main ingredients of B-LSSM are summarized briefly, including the superpotential, the general soft breaking terms, the Higgs sector and so on. Section 3 contains the effective Hamilton for $\bar{B} \to X_s\gamma$ and $B_s^0 \to \mu^+\mu^-$. The numerical analyses are given in Sect. 4, and Sect. 5 gives a summary. The tedious formulae are collected in Appendices.

2 The B-LSSM

In the B-LSSM, one enlarges the local gauge group of the SM to $SU(3)_C \otimes SU(2)_L \otimes U(1)_Y \otimes U(1)_{B-L}$, where the $U(1)_{B-L}$ can be spontaneously broken by the chiral singlet superfields $\hat{\eta}_1$ and $\hat{\eta}_2$. In literatures there are several popular versions of B-LSSM. Here we adopt the version described in Refs. [66–69] to proceed our analysis, and this version of B-LSSM is encoded in SARAH [70–74] which is used to create the mass matrices and interaction vertexes of the model. Besides the superfields of the MSSM, the exotic superfields of the B-LSSM are three generations of right-handed neutrinos $\hat{\nu}_i^c$ $\sim$(1, 1, 0, 1) and two chiral singlet superfields $\hat{\eta}_1 \sim (1, 1, 0, -1)$, $\hat{\eta}_2 \sim (1, 1, 0, 1)$. Meanwhile, quantum numbers of the matter chiral superfields for quarks and leptons are given by

$$\begin{aligned}
&\hat{Q}_i = \begin{pmatrix} \hat{U}_i \\ \hat{D}_i \end{pmatrix} \sim (3, 2, 1/6, 1/6),\\
&\hat{L}_i = \begin{pmatrix} \hat{\nu}_i \\ \hat{E}_i \end{pmatrix} \sim (1, 2, -1/2, -1/2),\\
&\hat{U}_i^c \sim (3, 1, -2/3, -1/6),\\
&\hat{D}_i^c \sim (3, 1, 1/3, -1/6), \quad \hat{E}_i^c \sim (1, 1, 1, 1/2),
\end{aligned} \tag{3}$$

with $i = 1, 2, 3$ denoting the index of generation. In addition, the quantum numbers of two Higgs doublets are assigned as

$$\begin{aligned}
&\hat{H}_1 = \begin{pmatrix} H_1^1 \\ H_1^2 \end{pmatrix} \sim (1, 2, -1/2, 0),\\
&\hat{H}_2 = \begin{pmatrix} H_2^1 \\ H_2^2 \end{pmatrix} \sim (1, 2, 1/2, 0).
\end{aligned} \tag{4}$$

The corresponding superpotential of the B-LSSM is written as

$$W = W_{MSSM} + W_{(B-L)}. \tag{5}$$

Here, W_{MSSM} is the superpotential of the MSSM, and $W_{(B-L)}$ is the sector involving exotic superfields,

$$W_{(B-L)} = Y_{v,ij}\hat{L}_i\hat{H}_2\hat{\nu}_j^c - \mu'\hat{\eta}_1\hat{\eta}_2 + Y_{x,ij}\hat{\nu}_i^c\hat{\eta}_1\hat{\nu}_j^c, \tag{6}$$

where i, j are generation indices. Correspondingly, the soft breaking terms of the B-LSSM are generally given as

$$\begin{aligned}
\mathcal{L}_{soft} = \mathcal{L}_{MSSM} + \Big[&-M_{BB'}\tilde{\lambda}_{B'}\tilde{\lambda}_B - \frac{1}{2}M_{B'}\tilde{\lambda}_{B'}\tilde{\lambda}_{B'}\\
&- B_{\mu'}\tilde{\eta}_1\tilde{\eta}_2 + T_v^{ij}H_2\tilde{\nu}_i^c\tilde{L}_j + T_x^{ij}\tilde{\eta}_1\tilde{\nu}_i^c\tilde{\nu}_j^c\\
&+ h.c.\Big] - m_{\tilde{\eta}_1}^2|\tilde{\eta}_1|^2 - m_{\tilde{\eta}_2}^2|\tilde{\eta}_2|^2 - m_{\tilde{\nu},ij}^2(\tilde{\nu}_i^c)^*\tilde{\nu}_j^c,
\end{aligned} \tag{7}$$

with λ_B, $\lambda_{B'}$ denoting the gaugino of $U(1)_Y$ and $U(1)_{(B-L)}$, respectively. $\mathcal{L}_{MSSM}$ is the soft breaking terms of the MSSM.

The presence of two Abelian groups gives rise to a new effect absent in the MSSM or other SUSY models with just one Abelian gauge group: the gauge kinetic mixing. It results from the invariance principle which allows the Lagrangian to include a mixing term between the strength tensors of gauge fields associated with the $U(1)$ gauge groups, $-\kappa_{Y,BL}A'^{Y}_{\mu}A'^{\mu,BL}$. Here, A'^{Y}_{μ}, $A'^{\mu,BL}$ denote the gauge fields associated with the two $U(1)$ gauge groups, $\kappa_{Y,BL}$ is an antisymmetric tensor which includes the mixing of $U(1)_Y$ and $U(1)_{B-L}$ gauge fields. This mixing couples the $B-L$ sector to the MSSM sector, and even if it is set to zero at M_{GUT}, it can be induced through renormalization group equations (RGEs) [75–81]. In practice, it turns out that it is easier to work with non-canonical covariant derivatives instead of off-diagonal field-strength tensors. However, both approaches are equivalent [82]. Hence in the following, we consider covariant derivatives of the form

$$D_\mu = \partial_\mu - i\left(Y,\ B-L\right)\begin{pmatrix} g_Y, & g'_{YB} \\ g'_{BY}, & g_{B-L} \end{pmatrix}\begin{pmatrix} A'^{Y}_{\mu} \\ A'^{BL}_{\mu} \end{pmatrix}, \tag{8}$$

where Y, $B-L$ corresponding to the hypercharge and $B-L$ charge respectively. As long as the two Abelian gauge groups are unbroken, we still have the freedom to perform a change of the basis

$$D_\mu = \partial_\mu - i\left(Y,\ B-L\right)\begin{pmatrix} g_Y, & g'_{YB} \\ g'_{BY}, & g_{B-L} \end{pmatrix}R^T R\begin{pmatrix} A'^{Y}_{\mu} \\ A'^{BL}_{\mu} \end{pmatrix}, \tag{9}$$

where R is a 2×2 orthogonal matrix. Choosing R in a proper form, one can write the coupling matrix as

$$\begin{pmatrix} g_Y, & g'_{YB} \\ g'_{BY}, & g_{B-L} \end{pmatrix}R^T = \begin{pmatrix} g_1, & g_{YB} \\ 0, & g_B \end{pmatrix}, \tag{10}$$

where g_1 corresponds to the measured hypercharge coupling which is modified in B-LSSM as given along with g_B and g_{YB} in Ref. [83]. In addition, we can redefine the $U(1)$ gauge fields

$$R\begin{pmatrix} A'^{Y}_{\mu} \\ A'^{BL}_{\mu} \end{pmatrix} = \begin{pmatrix} A^{Y}_{\mu} \\ A^{BL}_{\mu} \end{pmatrix}. \tag{11}$$

The local gauge symmetry $SU(2)_L \otimes U(1)_Y \otimes U(1)_{B-L}$ breaks down to the electromagnetic symmetry $U(1)_{em}$ as the Higgs fields receive vacuum expectation values (VEVs):

$$\begin{aligned} H_1^1 &= \frac{1}{\sqrt{2}}(v_1 + \mathrm{Re}H_1^1 + i\,\mathrm{Im}H_1^1), \\ H_2^2 &= \frac{1}{\sqrt{2}}(v_2 + \mathrm{Re}H_2^2 + i\,\mathrm{Im}H_2^2), \\ \tilde{\eta}_1 &= \frac{1}{\sqrt{2}}(u_1 + \mathrm{Re}\tilde{\eta}_1 + i\,\mathrm{Im}\tilde{\eta}_1), \\ \tilde{\eta}_2 &= \frac{1}{\sqrt{2}}(u_2 + \mathrm{Re}\tilde{\eta}_2 + i\,\mathrm{Im}\tilde{\eta}_2). \end{aligned} \tag{12}$$

For convenience, we define $u^2 = u_1^2 + u_2^2$, $v^2 = v_1^2 + v_2^2$ and $\tan\beta' = \frac{u_2}{u_1}$ in analogy to the ratio of the MSSM VEVs ($\tan\beta = \frac{v_2}{v_1}$). Meanwhile, the charged and neutral gauge bosons acquire the nonzero masses as

$$\begin{aligned} m_W^2 &= \frac{1}{4}g_2^2 v^2, \\ m_{Z,Z'}^2 &= \frac{1}{8}\Big[(g_1^2 + g_2^2 + g_{YB}^2)v^2 + 4g_B^2 u^2 \\ &\quad \mp \sqrt{(g_1^2 + g_2^2 + g_{YB}^2)^2 v^4 + 8(g_{YB}^2 - g_1^2 - g_2^2)g_B^2 v^2 u^2 + 16 g_B^4 u^4}\Big]. \end{aligned} \tag{13}$$

Compared the MSSM, this new gauge boson Z' makes new contribution to the process $B_s^0 \to \mu^+\mu^-$. In addition, the charged Higgs mass can be written as

$$M_{H^\pm}^2 = \frac{4B_\mu(1+\tan\beta^2) + g_2^2 v_1^2 \tan\beta(1+\tan\beta^2)}{4\tan\beta}. \tag{14}$$

In the basis ($\mathrm{Re}H_1^1$, $\mathrm{Re}H_2^2$, $\mathrm{Re}\tilde{\eta}_1$, $\mathrm{Re}\tilde{\eta}_2$), the tree level mass squared matrix for Higgs bosons is given by

$$M_h^2 = u^2 \times \begin{pmatrix} \frac{1}{4}\frac{g^2x^2}{1+\tan\beta^2} + n^2\tan\beta & -\frac{1}{4}g^2\frac{x^2\tan\beta}{1+\tan^2\beta} - n^2 & \frac{1}{2}g_B g_{YB}\frac{x}{T} & -\frac{1}{2}g_B g_{YB}\frac{x\tan\beta'}{T} \\ -\frac{1}{4}g^2\frac{x^2\tan\beta}{1+\tan^2\beta} - n^2 & \frac{1}{4}\frac{g^2\tan^2\beta x^2}{1+\tan\beta^2} + \frac{n^2}{\tan\beta} & \frac{1}{2}g_B g_{YB}\frac{x\tan\beta}{T} & \frac{1}{2}g_B g_{YB}\frac{x\tan\beta\tan\beta'}{T} \\ \frac{1}{2}g_B g_{YB}\frac{x}{T} & \frac{1}{2}g_B g_{YB}\frac{x\tan\beta}{T} & \frac{g_B^2}{1+\tan^2\beta'} + \tan\beta' N^2 & -g_B^2\frac{\tan\beta'}{1+\tan^2\beta'} - N^2 \\ -\frac{1}{2}g_B g_{YB}\frac{x\tan\beta'}{T} & \frac{1}{2}g_B g_{YB}\frac{x\tan\beta\tan\beta'}{T} & -g_B^2\frac{\tan\beta'}{1+\tan^2\beta'} - N^2 & g_B^2\frac{\tan^2\beta'}{1+\tan^2\beta'} + \frac{N^2}{\tan\beta'} \end{pmatrix}, \tag{15}$$

where $g^2 = g_1^2 + g_2^2 + g_{YB}^2$, $T = \sqrt{1+\tan^2\beta}\sqrt{1+\tan^2\beta'}$, $n^2 = \frac{\mathrm{Re}B\mu}{u^2}$, $N^2 = \frac{\mathrm{Re}B\mu'}{u^2}$, and $x = \frac{v}{u}$, respectively. These new extra singlets $\tilde{\eta}_{1,2}$ and the corresponding pseudo-scalar Higgs boson make new contributions to the process $B_s^0 \to \mu^+\mu^-$, with respect to the MSSM.

Including the leading-log radiative corrections from stop and top particles, the mass of the SM-like Higgs boson can be written as [84–86]

$$\begin{aligned} \Delta m_h^2 &= \frac{3m_t^4}{2\pi v^2}\left[\left(\tilde{t} + \frac{1}{2} + \tilde{X}_t\right)\right. \\ &\quad \left. + \frac{1}{16\pi^2}\left(\frac{3m_t^2}{2v^2} - 32\pi\alpha_3\right)\left(\tilde{t}^2 + \tilde{X}_t\tilde{t}\right)\right], \\ \tilde{t} &= log\frac{M_S^2}{m_t^2}, \qquad \tilde{X}_t = \frac{2\tilde{A}_t^2}{M_S^2}\left(1 - \frac{\tilde{A}_t^2}{12M_S^2}\right), \end{aligned} \tag{16}$$

where α_3 is the strong coupling constant, $M_S = \sqrt{m_{\tilde{t}_1}m_{\tilde{t}_2}}$ with $m_{\tilde{t}_{1,2}}$ denoting the stop masses, $\tilde{A}_t = A_t - \mu\cot\beta$ with $A_t = T_{u,33}$ being the trilinear Higgs stop coupling and μ denoting the Higgsino mass parameter. Then the SM-like Higgs mass can be written as

$$m_h = \sqrt{(m_{h_1}^0)^2 + \Delta m_h^2}, \tag{17}$$

where $m_{h_1}^0$ denotes the lightest tree-level Higgs boson mass.

Meanwhile, due to the gauge kinetic mixing, additional D-terms contribute to the mass matrices of the squarks and sleptons, and up type squarks affect the subsequent analysis. On the basis $(\tilde{u}_L, \tilde{u}_R)$, the mass matrix of up type squarks can be written as

$$m_{\tilde{u}}^2 = \begin{pmatrix} m_{uL}^2, & \frac{1}{\sqrt{2}}(v_2 T_u^\dagger - v_1\mu Y_u^\dagger) \\ \frac{1}{\sqrt{2}}(v_2 T_u - v_1\mu^* Y_u), & m_{uR}^2 \end{pmatrix}, \tag{18}$$

where,

$$\begin{aligned} m_{uL}^2 &= m_{\tilde{q}}^2 + \frac{1}{24}\Big[2g_B(g_B + g_{YB})(u_2^2 - u_1^2) \\ &\quad + g_{YB}(g_B + g_{YB})(v_2^2 - v_1^2) \\ &\quad + (-3g_2^2 + g_1^2)(v_2^2 - v_1^2)\Big] + \frac{v_2^2}{2}Y_u^\dagger Y_u, \end{aligned}$$

$$m^2_{uR} = m^2_{\tilde{u}} + \frac{1}{24}\Big[g_B(g_B + 4g_{YB})(u_1^2 - u_2^2) + g_{YB}(g_B + 4g_{YB})(v_1^2 - v_2^2) + 4g_1^2(v_1^2 - v_2^2)\Big] + \frac{v_1^2}{2}Y_u^\dagger Y_u. \quad (19)$$

It can be noted that $\tan\beta'$ and new gauge coupling constants g_B, g_{YB} in the B-LSSM can affect the mass matrix of up type squarks. Since up type squarks appear in the loops of the processes $\bar{B} \to X_s\gamma$ and $B_s^0 \to \mu^+\mu^-$, new definition of them affects the predictions of $Br(\bar{B} \to X_s\gamma)$ and $Br(B_s^0 \to \mu^+\mu^-)$ by influencing their masses and the corresponding couplings.

3 Theoretical calculation on $Br(\bar{B} \to X_s\gamma)$ and $Br(B_s^0 \to \mu^+\mu^-)$

The effective Hamilton for the transition $b \to s$ at hadronic scale can be written as

$$H_{eff} = -\frac{4G_F}{\sqrt{2}}V_{ts}^*V_{tb}\Bigg[C_1\mathcal{O}_1^c + C_2\mathcal{O}_2^c + \sum_{i=3}^{6}\mathcal{O}_i + \sum_{i=7}^{10}(C_i\mathcal{O}_i + C_i'\mathcal{O}_i') + \sum_{i=S,P}(C_i\mathcal{O}_i + C_i'\mathcal{O}_i')\Bigg], \quad (20)$$

where $\mathcal{O}_i (i = 1, 2, \ldots, 10, S, P)$ and $\mathcal{O}_i' (i = 7, 8, \ldots, 10, S, P)$ are defined as [87–92]

$$\mathcal{O}_1^u = (\bar{s}_L\gamma_\mu T^a u_L)(\bar{u}_L\gamma^\mu T^a b_L),$$
$$\mathcal{O}_2^u = (\bar{s}_L\gamma_\mu u_L)(\bar{u}_L\gamma^\mu b_L),$$
$$\mathcal{O}_3 = (\bar{s}_L\gamma_\mu b_L)\sum_q(\bar{q}\gamma^\mu q),$$
$$\mathcal{O}_4 = (\bar{s}_L\gamma_\mu T^a b_L)\sum_q(\bar{q}\gamma^\mu T^a q),$$
$$\mathcal{O}_5 = (\bar{s}_L\gamma_\mu\gamma_\nu\gamma_\rho b_L)\sum_q(\bar{q}\gamma^\mu\gamma^\nu\gamma^\rho q),$$
$$\mathcal{O}_6 = (\bar{s}_L\gamma_\mu\gamma_\nu\gamma_\rho T^a b_L)\sum_q(\bar{q}\gamma^\mu\gamma^\nu\gamma^\rho T^a q),$$
$$\mathcal{O}_7 = \frac{e}{16\pi^2}m_b(\bar{s}_L\sigma_{\mu\nu}b_R)F^{\mu\nu},$$
$$\mathcal{O}_7' = \frac{e}{16\pi^2}m_b(\bar{s}_R\sigma_{\mu\nu}b_L)F^{\mu\nu},$$
$$\mathcal{O}_8 = \frac{g_s}{16\pi^2}m_b(\bar{s}_L\sigma_{\mu\nu}T^a b_R)G^{a,\mu\nu},$$
$$\mathcal{O}_8' = \frac{g_s}{16\pi^2}m_b(\bar{s}_R\sigma_{\mu\nu}T^a b_L)G^{a,\mu\nu},$$
$$\mathcal{O}_9 = \frac{e^2}{g_s^2}(\bar{s}_L\gamma_\mu b_L)\bar{l}\gamma^\mu l, \quad \mathcal{O}_9' = \frac{e^2}{g_s^2}(\bar{s}_R\gamma_\mu b_R)\bar{l}\gamma^\mu l,$$
$$\mathcal{O}_{10} = \frac{e^2}{g_s^2}(\bar{s}_L\gamma_\mu b_L)\bar{l}\gamma^\mu\gamma_5 l, \quad \mathcal{O}_{10}' = \frac{e^2}{g_s^2}(\bar{s}_R\gamma_\mu b_R)\bar{l}\gamma^\mu\gamma_5 l,$$
$$\mathcal{O}_S = \frac{e^2}{16\pi^2}m_b(\bar{s}_L b_R)\bar{l}l, \quad \mathcal{O}_S' = \frac{e^2}{16\pi^2}m_b(\bar{s}_R b_L)\bar{l}l,$$
$$\mathcal{O}_P = \frac{e^2}{16\pi^2}m_b(\bar{s}_L b_R)\bar{l}\gamma_5 l,$$
$$\mathcal{O}_P' = \frac{e^2}{16\pi^2}m_b(\bar{s}_R b_L)\bar{l}\gamma_5 l, \quad (21)$$

where g_s denotes the strong coupling, $F^{\mu\nu}$ are the electromagnetic field strength tensors, $G^{\mu\nu}$ are the gluon field strength tensors, T^a $(a = 1, \ldots, 8)$ are $SU(3)$ generators.

3.1 Rare decay $\bar{B} \to X_s\gamma$

Compared with the SM, the main one loop Feynman diagrams contributing to the process $\bar{B} \to X_s\gamma$ in the B-LSSM are shown in Fig. 1. The picture shows that, new definition of the up type squarks affects the prediction of the process $\bar{B} \to X_s\gamma$, with respect to the MSSM. In addition, since the two loop electroweak corrections from closed squark loop are highly suppressed by heavy squark masses, we consider the corrections from closed fermion loop, and the corresponding Feynman diagrams are shown in Fig. 2. From the picture, we can see that, compared with the MSSM, new neutralinos in the B-LSSM make contributions to the process $\bar{B} \to X_s\gamma$.

Furthermore, the two loop diagrams which dressing the one loop diagrams in Fig. 1 with photon or Z boson exchange can also make contributions to the process. However, the contributions from these diagrams are suppressed, since the contributions from the two loop diagrams which dressing Fig. 1(3, 4) with photon or Z boson exchange are suppressed by heavy squark masses, we take Fig. 3 as an example to illustrate this point. Firstly, the contributions from the picture are suppressed by the factor $\frac{e^2}{(4\pi)^2}$, where e^2 comes from the interaction vertex, and $\frac{1}{(4\pi)^2}$ comes from the two loop momentum integral, which can be seen directly in Appendix A. Secondly, according to the decoupling theorem, the contributions from the picture are suppressed by $\frac{\Lambda_{EW}^2}{\Lambda^2}$. Then in our chosen parameter space, the corrections from Fig. 3 to $Br(\bar{B} \to X_s\gamma)$ can only reach 0.1%. Similarly, the two loop diagrams which dressing Fig. 1 with Z boson exchanges are also suppressed, because compared with Fig. 3, these diagrams just replace the electromagnetic interaction to smaller weak interaction. Hence we neglect the contributions from all of these diagrams.

Then the branching ratio of $\bar{B} \to X_s\gamma$ in the B-LSSM can be written as

$$Br(\bar{B} \to X_s\gamma) = R\left(|C_{7\gamma}(\mu_b)|^2 + N(E_\gamma)\right), \quad (22)$$

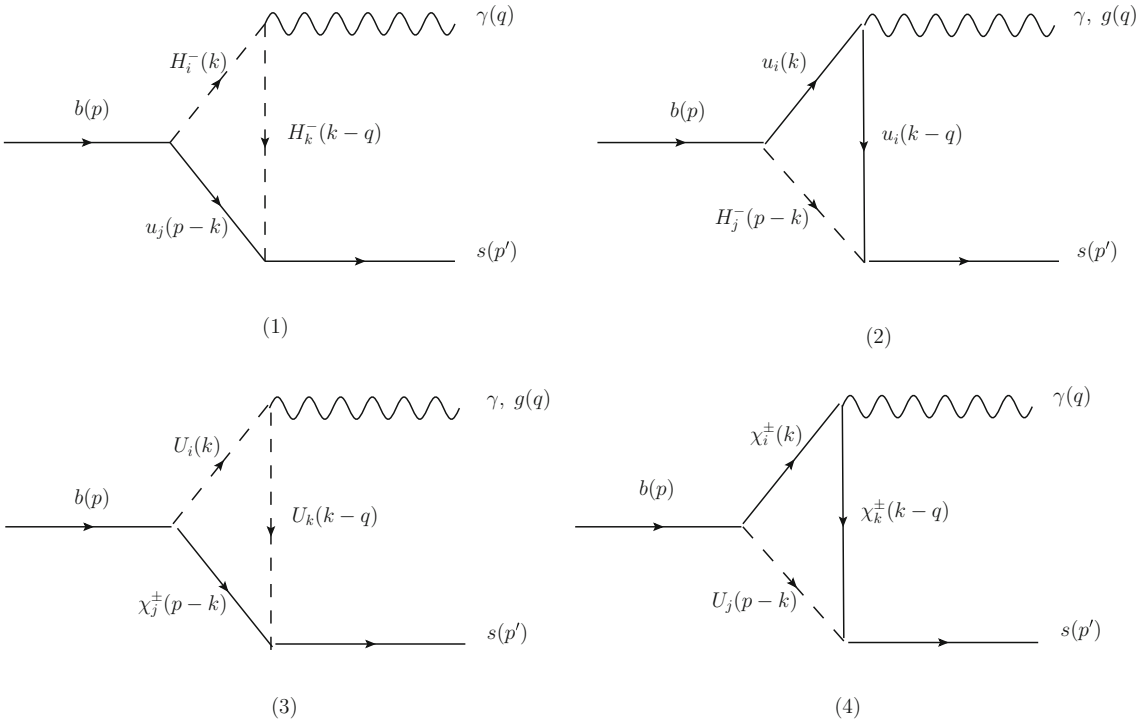

Fig. 1 The one loop Feynman diagrams contributing to $\bar{B} \to X_s\gamma$ from exotic fields in the B-LSSM

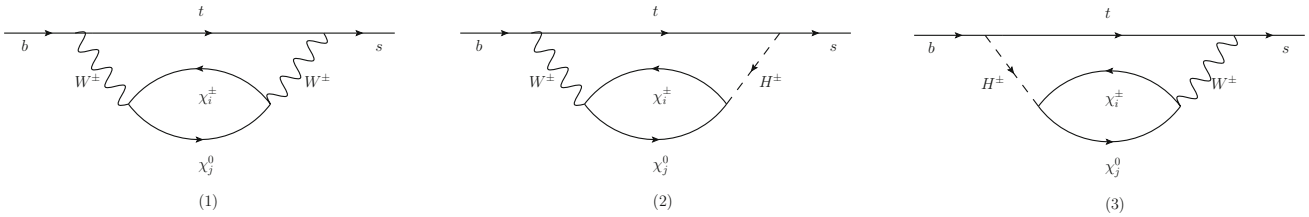

Fig. 2 The relating two loop diagrams in which a closed heavy fermion loop is attached to virtual $W^\pm$ bosons or $H^\pm$, where a real photon or gluon is attached in all possible ways

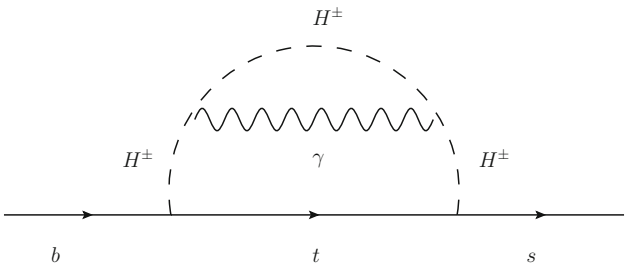

Fig. 3 The two loop diagram which dressing Fig. 1a with photon exchanges, where a real photon or gluon is attached in all possible ways

where the overall factor $R = 2.47 \times 10^{-3}$, and the nonperturbative contribution $N(E_\gamma) = (3.6 \pm 0.6) \times 10^{-3}$ [93]. $C_{7\gamma}(\mu_b)$ is defined by

$$C_{7\gamma}(\mu_b) = C_{7\gamma,SM}(\mu_b) + C_{7,NP}(\mu_b), \tag{23}$$

where we choose the hadron scale $\mu_b = 2.5\,\text{GeV}$ and use the SM contribution at NNLO level $C_{7\gamma,SM}(\mu_b) = -0.3689$ [93–96]. The Wilson coefficients for new physics at the bottom quark scale can be written as [97,98]

$$\begin{aligned} C_{7,NP}(\mu_b) \approx\ & 0.5696 C_{7,NP}(\mu_{EW}) \\ & + 0.1107 C_{8,NP}(\mu_{EW}), \end{aligned} \tag{24}$$

where

$$\begin{aligned} C_{7,NP}^{NP}(\mu_{EW}) =\ & C_{7,NP}^{(1)}(\mu_{EW}) + C_{7,NP}^{(2)}(\mu_{EW}) \\ & + C_{7,NP}^{(3)}(\mu_{EW}) + C_{7,NP}^{(4)}(\mu_{EW}) \\ & + C_{7,NP}^{\prime(1)}(\mu_{EW}) + C_{7,NP}^{\prime(2)}(\mu_{EW}) \\ & + C_{7,NP}^{\prime(3)}(\mu_{EW}) + C_{7,NP}^{\prime(4)}(\mu_{EW}) \\ & + C_{7,NP}^{WW}(\mu_{EW}) + C_{7,NP}^{WH}(\mu_{EW}), \\ C_{8,NP}(\mu_{EW}) =\ & C_{8g,NP}(\mu_{EW}) + C_{8g,NP}^{\prime}(\mu_{EW}) \\ & + C_{8,NP}^{WW}(\mu_{EW}) + C_{8,NP}^{WH}(\mu_{EW}), \end{aligned} \tag{25}$$

where $C_{7,NP}^{(1,\ldots,4)}(\mu_{EW})$, $C_{7,NP}^{WW}(\mu_{EW})$, $C_{7,NP}^{WH}(\mu_{EW})$ are Wilson coefficients of the process $b \to s\gamma$ corresponding

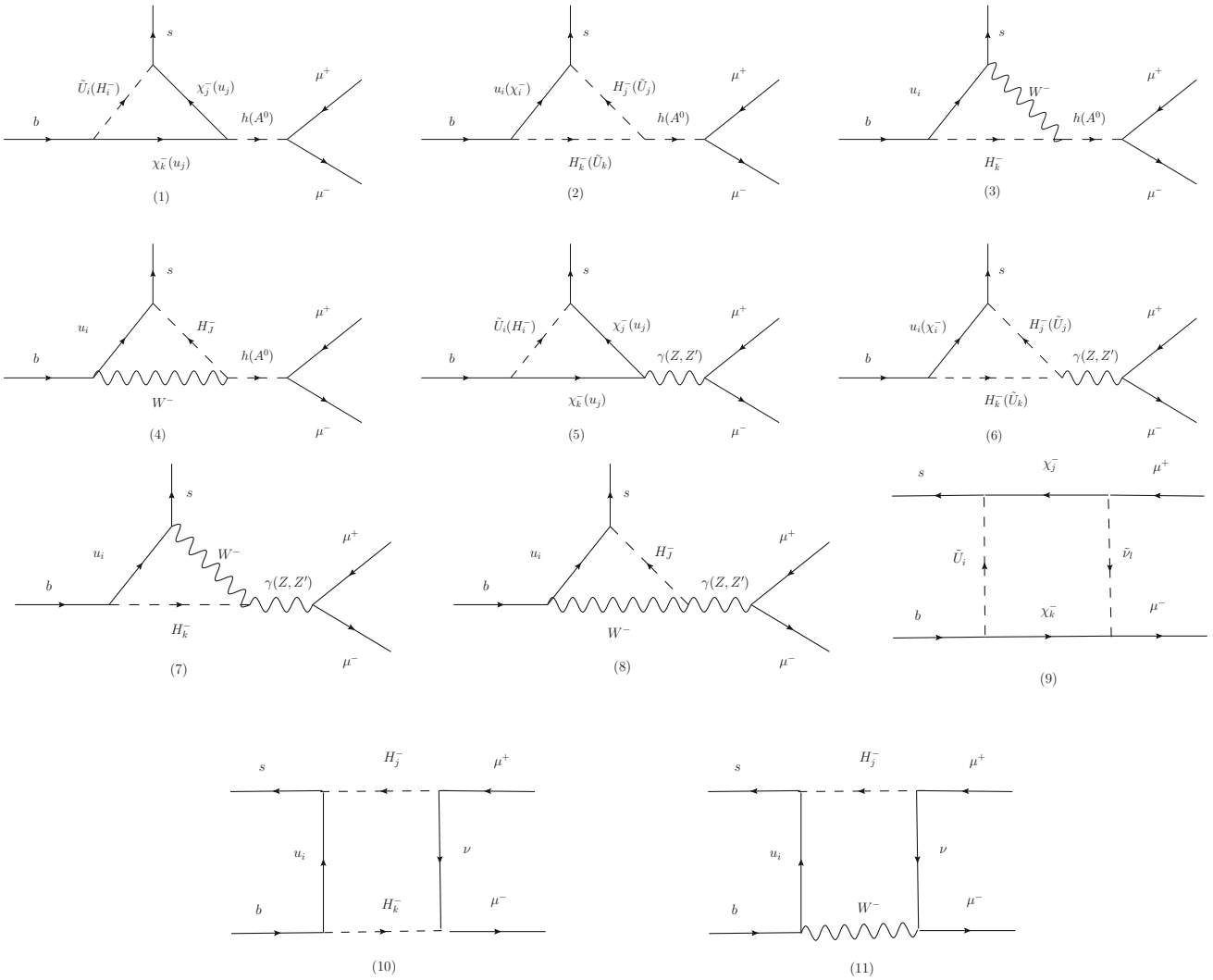

Fig. 4 The Feynman diagrams contributing to the decay $B_s^0 \to \mu^+\mu^-$ in the B-LSSM

to Figs. 1, 2, and the concrete expressions are collected in Appendix B. Equation (B3) indicates that the corrections to the Wilson coefficients from Fig. 2(2, 3) are suppressed. In addition, $C_{8g,NP}(\mu_{EW})$, $C'_{8g,NP}(\mu_{EW})$, $C^{WW}_{8,NP}(\mu_{EW})$, $C^{WH}_{8,NP}(\mu_{EW})$ are Wilson coefficients of the process $b \to sg$ in the B-LSSM, where $C_{8g,NP}(\mu_{EW})$, $C'_{8g,NP}(\mu_{EW})$ denote the QCD corrections to the one loop contributions in Fig. 1. Then $C_{8g,NP}(\mu_{EW})$ and $C'_{8g,NP}(\mu_{EW})$ at electroweak scale are

$$\begin{aligned} C_{8g,NP}(\mu_{EW}) &= [C^{(2)}_{7,NP}(\mu_{EW}) + C^{(3)}_{7,NP}(\mu_{EW})]/Q_u \\ &\quad + C^{WW}_{8,NP}(\mu_{EW}) + C^{WH}_{8,NP}(\mu_{EW}), \\ C'_{8g,NP}(\mu_{EW}) &= C_{8g,NP}(\mu_{EW})(L \leftrightarrow R), \end{aligned} \tag{26}$$

where $Q_u = 2/3$. And the concrete expressions of $C^{WW}_{8,NP}(\mu_{EW})$, $C^{WH}_{8,NP}(\mu_{EW})$ are collected in Appendix B. Compared with the MSSM, new neutralinos make contributions to the process $\bar{B} \to X_s\gamma$. In addition, $\tan\beta'$, g_B and gauge kinetic mixing g_{YB} in the B-LSSM might influence the theoretical prediction on $Br(\bar{B} \to X_s\gamma)$ through affecting the up type squarks masses and the corresponding couplings.

3.2 Rare decay $B_s^0 \to \mu^+\mu^-$

The main Feynman diagrams contributing to the process $B_s^0 \to \mu^+\mu^-$ in the B-LSSM are shown in Fig. 4. Compared with the MSSM, Fig. 4 shows that new definition of up type squarks, new gauge boson Z', new scalar and pseudoscalar Higgs bosons make new contributions to the processes $B_s^0 \to \mu^+\mu^-$ in the B-LSSM. In addition, since the contributions from Fig. 2(2, 3) are suppressed, we also consider the two loop electroweak corrections from Fig. 2(1), a virtual photon, Z boson or Z' boson is attached in all possible ways. And for the same reason as the process $\bar{B} \to X_s\gamma$, we neglect the contributions from the two loop diagrams which dressing Fig. 4 with γ or Z exchange. At the electroweak energy scale μ_{EW}, the corresponding Wilson coefficients can be written as

$$
\begin{aligned}
C_{S,NP}(\mu_{\rm EW}) &= \frac{\sqrt{2}s_W c_W}{4m_b e^3 V_{ts}^* V_{tb}}\Big[C_{S,NP}^{(1)}(\mu_{\rm EW}) + C_{S,NP}^{(2)}(\mu_{\rm EW}) \\
&\quad + C_{S,NP}^{(3)}(\mu_{\rm EW}) + C_{S,NP}^{(4)}(\mu_{\rm EW}) + C_{S,NP}^{(6)}(\mu_{\rm EW}) \\
&\quad + C_{S,NP}^{(9)}(\mu_{\rm EW}) + C_{S,NP}^{(11)}(\mu_{\rm EW})\Big], \\
C'_{S,NP}(\mu_{\rm EW}) &= C_{S,NP}(\mu_{\rm EW})(L \leftrightarrow R), \\
C_{P,NP}(\mu_{\rm EW}) &= \frac{\sqrt{2}s_W c_W}{4m_b e^3 V_{ts}^* V_{tb}}\Big[C_{P,NP}^{(1)}(\mu_{\rm EW}) + C_{P,NP}^{(2)}(\mu_{\rm EW}) \\
&\quad + C_{P,NP}^{(3)}(\mu_{\rm EW}) + C_{P,NP}^{(4)}(\mu_{\rm EW}) + C_{P,NP}^{(6)}(\mu_{\rm EW}) \\
&\quad + C_{P,NP}^{(9)}(\mu_{\rm EW}) + C_{P,NP}^{(11)}(\mu_{\rm EW})\Big], \\
C'_{P,NP}(\mu_{\rm EW}) &= -C_{P,NP}(\mu_{\rm EW})(L \leftrightarrow R), \\
C_{9,NP}(\mu_{\rm EW}) &= \frac{\sqrt{2}s_W c_W g_s^2}{64\pi^2 e^3 V_{ts}^* V_{tb}}\Big[C_{9,NP}^{(5)}(\mu_{\rm EW}) + C_{9,NP}^{(6)}(\mu_{\rm EW}) \\
&\quad + C_{9,NP}^{(7)}(\mu_{\rm EW}) + C_{9,NP}^{(8)}(\mu_{\rm EW}) + C_{9,NP}^{(9)}(\mu_{\rm EW}) \\
&\quad + C_{9,NP}^{(10)}(\mu_{\rm EW}) + C_{9,NP}^{WW}(\mu_{\rm EW})\Big], \\
C'_{9,NP}(\mu_{\rm EW}) &= C_{9,NP}(\mu_{\rm EW})(L \leftrightarrow R), \\
C_{10,NP}(\mu_{\rm EW}) &= \frac{\sqrt{2}s_W c_W g_s^2}{64\pi^2 e^3 V_{ts}^* V_{tb}}\Big[C_{10,NP}^{(5)}(\mu_{\rm EW}) + C_{10,NP}^{(6)}(\mu_{\rm EW}) \\
&\quad + C_{10,NP}^{(7)}(\mu_{\rm EW}) + C_{10,NP}^{(8)}(\mu_{\rm EW}) + C_{10,NP}^{(9)}(\mu_{\rm EW}) \\
&\quad + C_{10,NP}^{(10)}(\mu_{\rm EW}) + C_{10,NP}^{WW}(\mu_{\rm EW})\Big], \\
C'_{10,NP}(\mu_{\rm EW}) &= -C_{10,NP}(\mu_{\rm EW})(L \leftrightarrow R). \qquad (27)
\end{aligned}
$$

Here, the superscripts $(1,\ldots,11,WW)$ corresponding to the new physics corrections in Figs. 2(1) and 4, the concrete expressions of these Wilson coefficients can be found in Appendix C, and all of the calculated corrections above are gauge invariant. Furthermore, the Wilson coefficients are calculated at the matching scale μ_{EW}, then evolved down to hadronic scale $\mu \sim m_b$ by the renormalization group equations. In order to obtain hadronic matrix elements conveniently, we define effective coefficients [89]

$$
\begin{aligned}
C_7^{eff} &= \frac{4\pi}{\alpha_s}C_7 - \frac{1}{3}C_3 - \frac{4}{9}C_4 - \frac{20}{3}C_5 - \frac{80}{9}C_6, \\
C_8^{eff} &= \frac{4\pi}{\alpha_s}C_8 + C_3 - \frac{1}{6}C_4 + 20C_5 - \frac{10}{3}C_6, \\
C_9^{eff} &= \frac{4\pi}{\alpha_s}C_9 + Y(q^2), \quad C_{10}^{eff} = \frac{4\pi}{\alpha_s}C_{10}, \\
C'^{eff}_{7,8,9,10} &= \frac{4\pi}{\alpha_s}C'_{7,8,9,10}. \qquad (28)
\end{aligned}
$$

The Wilson coefficients at hadronic energy scale from the SM to next-to-next-to-logarithmic (NNLL) accuracy are shown in Table 1. On the other hand, the renormalization group equations which evolve the matching scale down to hadronic scale can be written as

$$
\begin{aligned}
\vec{C}_{NP}(\mu) &= \widehat{U}(\mu,\mu_0)\vec{C}_{NP}(\mu_0), \\
\vec{C}'_{NP}(\mu) &= \widehat{U'}(\mu,\mu_0)\vec{C}'_{NP}(\mu_0) \qquad (29)
\end{aligned}
$$

with

$$
\begin{aligned}
\vec{C}^{\,T}_{NP} &= \Big(C_{1,NP},\ \ldots,\ C_{6,NP}, C_{7,NP}^{eff},\ C_{8,NP}^{eff},\ C_{9,NP}^{eff} \\
&\quad - Y(q^2),\ C_{10,NP}^{eff}\Big), \\
\vec{C}^{\,\prime,\,T}_{NP} &= \Big(C_{7,NP}^{\prime,\,eff},\ C_{8,NP}^{\prime,\,eff},\ C_{9,NP}^{\prime,\,eff},\ C_{10,NP}^{\prime,\,eff}\Big). \qquad (30)
\end{aligned}
$$

Correspondingly, the evolving matrices are approached as

$$
\begin{aligned}
\widehat{U}(\mu,\mu_0) &\simeq 1 - \left[\frac{1}{2\beta_0}\ln\frac{\alpha_s(\mu)}{\alpha_s(\mu_0)}\right]\widehat{\gamma}^{(0)T}, \\
\widehat{U'}(\mu,\mu_0) &\simeq 1 - \left[\frac{1}{2\beta_0}\ln\frac{\alpha_s(\mu)}{\alpha_s(\mu_0)}\right]\widehat{\gamma}'^{(0)T}, \qquad (31)
\end{aligned}
$$

where the anomalous dimension matrices can be read from Ref. [99] as

$$
\widehat{\gamma}^{(0)} = \begin{pmatrix}
-4 & \frac{8}{3} & 0 & -\frac{2}{9} & 0 & 0 & -\frac{208}{243} & \frac{173}{162} & -\frac{2272}{729} & 0 \\
12 & 0 & 0 & \frac{4}{3} & 0 & 0 & \frac{416}{81} & \frac{70}{27} & \frac{1952}{243} & 0 \\
0 & 0 & 0 & -\frac{52}{3} & 0 & 2 & -\frac{176}{81} & \frac{14}{27} & -\frac{6752}{243} & 0 \\
0 & 0 & -\frac{40}{9} & -\frac{100}{9} & \frac{4}{9} & \frac{5}{6} & -\frac{152}{243} & -\frac{587}{162} & -\frac{2192}{729} & 0 \\
0 & 0 & 0 & -\frac{256}{3} & 0 & 20 & -\frac{6272}{81} & \frac{6596}{27} & -\frac{84032}{243} & 0 \\
0 & 0 & -\frac{256}{9} & \frac{56}{9} & \frac{40}{9} & -\frac{2}{3} & \frac{4624}{243} & \frac{4772}{81} & -\frac{37856}{729} & 0 \\
0 & 0 & 0 & 0 & 0 & 0 & \frac{32}{3} & 0 & 0 & 0 \\
0 & 0 & 0 & 0 & 0 & 0 & -\frac{32}{9} & \frac{28}{3} & 0 & 0 \\
0 & 0 & 0 & 0 & 0 & 0 & 0 & 0 & 0 & 0 \\
0 & 0 & 0 & 0 & 0 & 0 & 0 & 0 & 0 & 0
\end{pmatrix}, \quad
\widehat{\gamma}'^{(0)} = \begin{pmatrix}
\frac{32}{3} & 0 & 0 & 0 \\
-\frac{32}{9} & \frac{28}{3} & 0 & 0 \\
0 & 0 & 0 & 0 \\
0 & 0 & 0 & 0
\end{pmatrix}. \qquad (32)
$$

Then, the squared amplitude can be written as

$$
|\mathcal{M}_s|^2 = 16G_F^2|V_{tb}V_{ts}^*|^2 M_{B_s^0}^2\Big[|F_S^s|^2 + |F_P^s + 2m_\mu F_A^s|^2\Big], \qquad (33)
$$

Table 1 At hadronic scale $\mu = m_b \simeq 4.65\,\text{GeV}$, SM Wilson coefficients to NNLL accuracy

$C_7^{eff,SM}$	$C_8^{eff,SM}$	$C_9^{eff,SM} - Y(q^2)$	$C_{10}^{eff,SM}$
−0.304	−0.167	4.211	−4.103

and

$$F_S^s = \frac{\alpha_{EW}(\mu_b)}{8\pi}\frac{m_b M_{B_s^0}^2}{m_b + m_s} f_{B_s^0}(C_S - C_S'), \tag{34}$$

$$F_P^s = \frac{\alpha_{EW}(\mu_b)}{8\pi}\frac{m_b M_{B_s^0}^2}{m_b + m_s} f_{B_s^0}(C_P - C_P'), \tag{35}$$

$$F_A^s = \frac{\alpha_{EW}(\mu_b)}{8\pi} f_{B_s^0}\left[C_{10}^{eff}(\mu_b) - C_{10}^{\prime eff}(\mu_b)\right], \tag{36}$$

where $f_{B_s^0} = (227 \pm 8)\,\text{MeV}$ denote the decay constants, $M_{B_s^0} = 5.367\,\text{GeV}$ denote the masses of neutral meson B_s^0.

The branching ratio of $B_s^0 \to \mu^+\mu^-$ can be written as

$$Br(B_s^0 \to \mu^+\mu^-) = \frac{\tau_{B_s^0}}{16\pi}\frac{|\mathcal{M}_s|^2}{M_{B_s^0}}\sqrt{1 - \frac{4m_\mu^2}{M_{B_s^0}^2}}, \tag{37}$$

with $\tau_{B_s^0} = 1.466(31)\text{ps}$ denoting the life time of meson.

4 Numerical analyses

In this section, we present the numerical results of the branching ratios of rare B-decays $\bar{B} \to X_s\gamma$ and $B_s^0 \to \mu^+\mu^-$. The relevant SM input parameters are chosen as $m_W = 80.385\,\text{GeV}$, $m_Z = 90.19\,\text{GeV}$, $\alpha_{em}(m_Z) = 1/128.9$, $\alpha_s(m_Z) = 0.118$, $m_b = 4.65\,\text{GeV}$, $m_s = 0.095\,\text{GeV}$. Since the tiny neutrino masses basically do not affect $Br(\bar{B} \to X_s\gamma)$ and $Br(B_s^0 \to \mu^+\mu^-)$, we take $Y_\nu = Y_x = 0$ approximately. The SM-like Higgs mass is [1]

$$m_h = 125.09 \pm 0.24\,\text{GeV}. \tag{38}$$

Meanwhile the CKM matrix is

$$\begin{pmatrix} 0.97417 & 0.2248 & 4.09\times10^{-3} \\ -0.22 & 0.995 & 4.05\times10^{-2} \\ 8.2\times10^{-3} & -4\times10^{-2} & 1.009 \end{pmatrix}. \tag{39}$$

The updated experimental data [100] on searching Z' indicates $M_{Z'} \geq 4.05\,\text{TeV}$ at 95% Confidence Level (CL). Due to the contributions of heavy Z' boson are highly suppressed, we choose $M_{Z'} = 4.2\,\text{TeV}$ in our following numerical analysis. And Refs. [101,102] give us an upper bound on the ratio between the $Z^{'}$ mass and its gauge coupling at 99% CL as

$$M_{Z'}/g_B \geq 6\,\text{TeV}. \tag{40}$$

Then the scope of g_B is limited to $0 < g_B \leq 0.7$. Additionally, the LHC experimental data also constrain $\tan\beta^{'} < 1.5$ [67]. Considering the constraints from the experiments [1], for those parameters in Higgsino and gaugino sectors, we appropriately fix $M_1 = 500\,\text{GeV}$, $M_2 = 600\,\text{GeV}$, $\mu = 700\,\text{GeV}$, $\mu^{'} = 800\,\text{GeV}$, $M_{BB'} = 500\,\text{GeV}$, $M_{BL} = 600\,\text{GeV}$, for simplify. For those parameters in the soft breaking terms, we set $B'_\mu = 5\times10^5\,\text{GeV}^2$, $m_{\tilde{l}} = m_{\tilde{e}} = T_\nu = T_x = diag(1,1,1)\,\text{TeV}$. In addition, the first two generations of squarks are strongly constrained by direct searches at the LHC [103,104] and the third generation squark masses are not constrained by the LHC as strong as the first two generations, and affect the SM-like Higgs mass. Therefore we take $m_{\tilde{q}} = m_{\tilde{u}} = diag(2,2,m_{\tilde{t}})\,\text{TeV}$, and the discission about the observed Higgs signal in Ref. [105] limits $m_{\tilde{t}} \gtrsim 1.5\,\text{TeV}$. For simplify, we also choose $T_{u_{1,2}} = 1\,\text{TeV}$. As a key parameter, $T_{u_3} = A_t$ affects SM-like Higgs mass and the following numerical calculation.

In the scenarios of the MSSM, the new physics contributions to the branching ratios of $\bar{B} \to X_s\gamma$ and $B_s^0 \to \mu^+\mu^-$ depend essentially on A_t, $\tan\beta$ and charged Higgs mass $M_{H^\pm}$. In order to see how A_t, $\tan\beta$, $M_{H^\pm}$ affect the theoretical evaluations of $Br(\bar{B} \to X_s\gamma)$ and $Br(B_s^0 \to \mu^+\mu^-)$ in the B-LSSM, we assume that $g_B = 0.4$, $g_{YB} = -0.5$, $\tan\beta' = 1.1$ in the following analysis. Then taking $m_{\tilde{t}} = 1.6\,\text{TeV}$, $M_{H^\pm} = 1.5\,\text{TeV}$, we plot $Br(\bar{B} \to X_s\gamma)$ and $Br(B_s^0 \to \mu^+\mu^-)$ versus A_t in Fig. 5, for $\tan\beta = 5$(solid line), $\tan\beta = 20$(dashed line) and $\tan\beta = 35$(dotted line), respectively. The gray area denotes the experimental 1σ bounds in Eq. (1). In Fig. 5a, we can see that $Br(\bar{B} \to X_s\gamma)$ decreases with the increasing of A_t, and $Br(\bar{B} \to X_s\gamma)$ will be easily coincides with experimental data within one standard deviation when A_t is positive. Meanwhile, Fig. 5b shows that $Br(B_s^0 \to \mu^+\mu^-)$ favor A_t in the ranges $-3.6\,\text{TeV} \lesssim A_t \lesssim 1.4\,\text{TeV}$ as $\tan\beta = 5$, $-1.2\,\text{TeV} \lesssim A_t \lesssim 0.2\,\text{TeV}$ as $\tan\beta = 20$ and $-0.8\,\text{TeV} \lesssim A_t \lesssim 0\,\text{TeV}$ as $\tan\beta = 35$, which also coincide with the experimental data on $Br(\bar{B} \to X_s\gamma)$. It can be noted that when $\tan\beta$ is large, the range of A_t is limited strongly by the experimental data on $Br(B_s^0 \to \mu^+\mu^-)$.

Then, in order to see the difference between two loop and one loop corrections to the processes, we take $\tan\beta = 20$, and plot $Br(\bar{B} \to X_s\gamma)$, $Br(B_s^0 \to \mu^+\mu^-)$ versus A_t in Fig. 6. The solid and dashed line denote two loop and one loop predictions respectively. Figure 6a shows that, the relative corrections from two loop diagrams to one loop corrections of $Br(\bar{B} \to X_s\gamma)$ can reach around 3%, which produces a more precise prediction on the process $\bar{B} \to X_s\gamma$, and we cannot neglect the corrections with this magnitude. In Fig. 6b, these two lines coincide with each other, which indicates the two loop corrections to $Br(B_s^0 \to \mu^+\mu^-)$ are negligible compared with the one loop corrections. In the

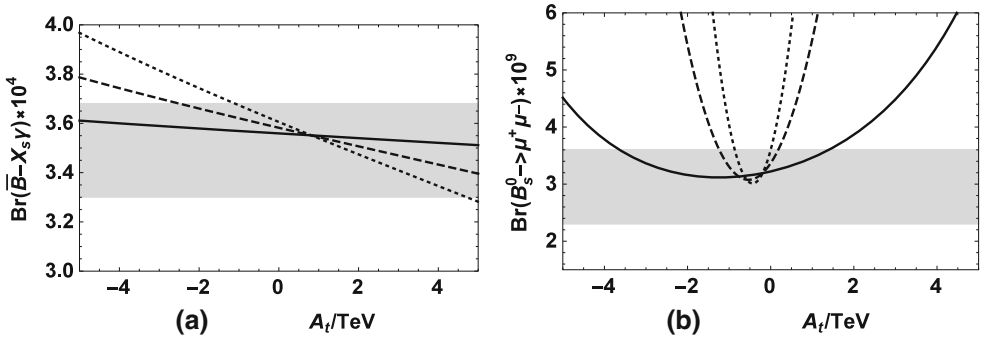

Fig. 5 $Br(\bar{B} \to X_s\gamma)$ (**a**) and $Br(B_s^0 \to \mu^+\mu^-)$ (**b**) versus A_t for $\tan\beta = 5$ (solid line), $\tan\beta = 20$ (dashed line), $\tan\beta = 35$ (dotted line), when $m_{\tilde{t}} = 1.6\,\text{TeV}$, $M_{H^\pm} = 1.5\,\text{TeV}$. The gray area denotes the experimental 1σ interval

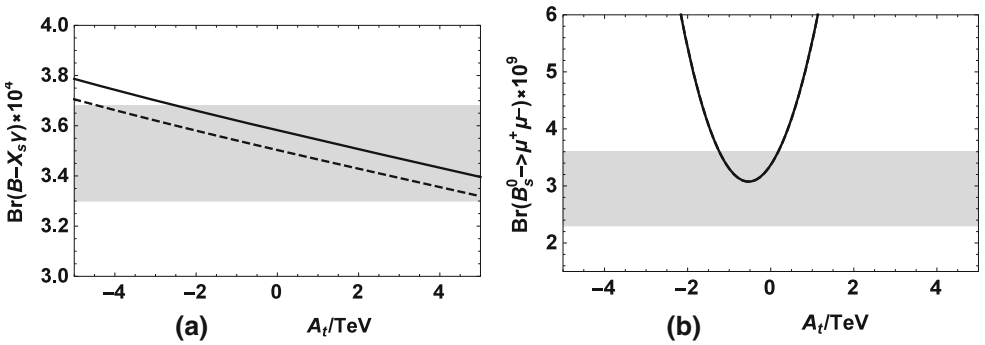

Fig. 6 $Br(\bar{B} \to X_s\gamma)$ (**a**) and $Br(B_s^0 \to \mu^+\mu^-)$ (**b**) versus A_t for two loop result (solid line) and one loop result (dashed line). The gray area denotes the experimental 1σ interval

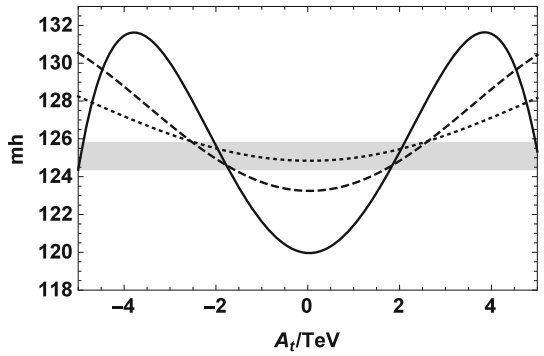

Fig. 7 Taking $\tan\beta = 20$, we plot the SM-like Higgs mass m_h versus A_t for $m_{\tilde{t}} = 1.5\,\text{TeV}$ (solid line), $m_{\tilde{t}} = 2.5\,\text{TeV}$ (dashed line) and $m_{\tilde{t}} = 3.5\,\text{TeV}$ (dotted line), where the gray area denotes the experimental 3σ interval

analysis of the numerical results, we use the more precise two loop predictions.

In addition, we also need to consider the constraint of the SM-like Higgs mass. Taking $\tan\beta = 20$, we plot the SM-like Higgs mass m_h versus A_t in Fig. 7 for $m_{\tilde{t}} = 1.5\,\text{TeV}$ (solid line), $m_{\tilde{t}} = 2.5\,\text{TeV}$ (dashed line) and $m_{\tilde{t}} = 3.5\,\text{TeV}$ (dotted line). The gray area denotes the experimental 3σ interval. To keep the SM-like Higgs mass around 125 GeV, we need $A_t \approx \pm 1.8\,\text{TeV}$ as $m_{\tilde{t}} = 1.5\,\text{TeV}$. When $m_{\tilde{t}} = 2.5\,\text{TeV}$, we require that A_t in the range $-2.5\,\text{TeV} \lesssim A_t \lesssim 1.6\,\text{TeV}$ or $1.6\,\text{TeV} \lesssim A_t \lesssim 2.5\,\text{TeV}$. And the allowed range of A_t is $-2.5\,\text{TeV} \lesssim A_t \lesssim 2.5\,\text{TeV}$ when $m_{\tilde{t}} = 3.5\,\text{TeV}$.

Since the large charged Higgs mass does not affect the SM-like Higgs mass signally, we can choose $A_t = -2.5\,\text{TeV}$, $-0.5\,\text{TeV}$ and $1.5\,\text{TeV}$ for $m_{\tilde{t}} = 3.5\,\text{TeV}$, to keep the SM-like Higgs mass around 125 GeV. Then we plot $Br(\bar{B} \to X_s\gamma)$ and $Br(B_s^0 \to \mu^+\mu^-)$ versus $M_{H^\pm}$ in Fig. 8, where the solid line, dashed line and dotted line denote $A_t = -2.5\,\text{TeV}$, $-0.5\,\text{TeV}$, $1.5\,\text{TeV}$, respectively. The gray area denotes the experimental 1σ bounds. It is obvious that A_t affect the numerical results negligibly compared with $M_{H^\pm}$, because large $m_{\tilde{t}}$ suppresses the effects of A_t. In addition, Fig. 8a shows that $Br(\bar{B} \to X_s\gamma)$ decreases along with the increasing of $M_{H^\pm}$, because the contributions from charged Higgs diagrams decay like $1/M_{H^\pm}^4$ [106]. And the experimental data on $Br(\bar{B} \to X_s\gamma)$ favor $M_{H^\pm}$ lying in the ranges $M_{H^\pm} \gtrsim 0.7\,\text{TeV}$. Meanwhile, in Fig. 8b, we can see that for small $M_{H^\pm}$, the new physics could contribute with large corrections to the branching ratio of $B_s^0 \to \mu^+\mu^-$, and the experimental data on $Br(B_s^0 \to \mu^+\mu^-)$ limits that $M_{H^\pm} \gtrsim 0.8\,\text{TeV}$.

In order to see the effects of g_B, g_{YB} and $\tan\beta'$ which are new parameters in the B-LSSM compared with MSSM, we take $\tan\beta = 20$, $m_{\tilde{t}} = 1.6\,\text{TeV}$, $A_t = -0.5\,\text{TeV}$, $M_{H^\pm} =$

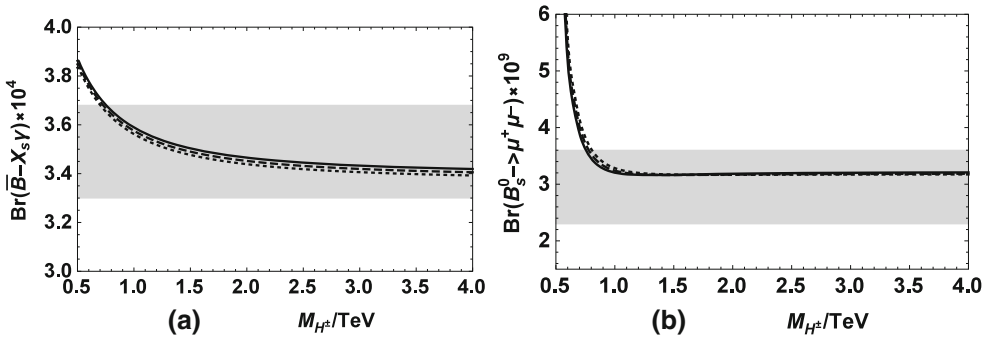

Fig. 8 $Br(\bar{B} \to X_s\gamma)$ (**a**) and $Br(B_s^0 \to \mu^+\mu^-)$ (**b**) versus $M_{H^\pm}$ for $A_t = -2.5\,\text{TeV}$ (solid line), $A_t = -0.5\,\text{TeV}$ (dashed line), $A_t = 1.5\,\text{TeV}$ (dotted line), when $\tan\beta = 20$, $m_{\tilde{t}} = 3.5\,\text{TeV}$. The gray area denotes the experimental 1σ interval

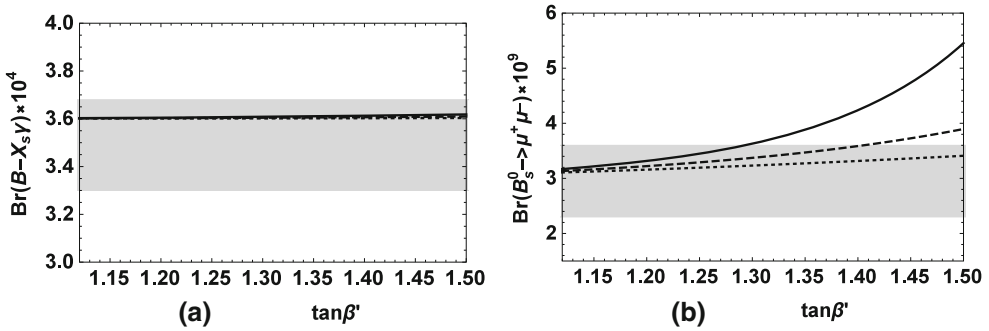

Fig. 9 $Br(\bar{B} \to X_s\gamma)$ (**a**) and $Br(B_s^0 \to \mu^+\mu^-)$ (**b**) versus $\tan\beta'$ for $g_{YB} = -0.6$ (solid line), $g_{YB} = -0.5$ (dashed line), $g_{YB} = -0.4$ (dotted line). The gray area denotes the experimental 1σ interval

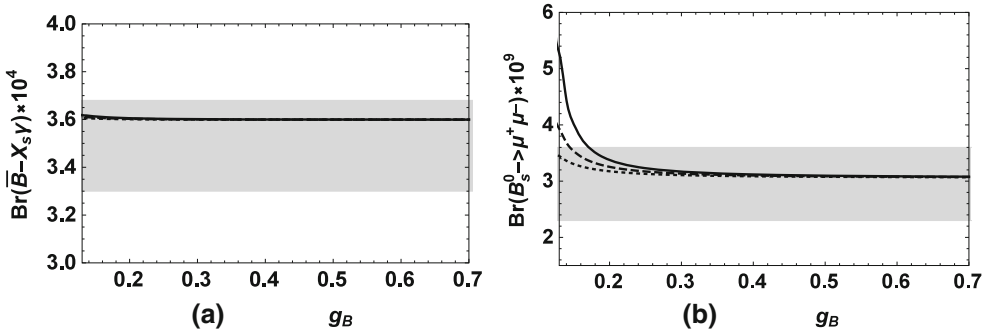

Fig. 10 $Br(\bar{B} \to X_s\gamma)$ (**a**) and $Br(B_s^0 \to \mu^+\mu^-)$ (**b**) versus g_B for $g_{YB} = -0.6$ (solid line), $g_{YB} = -0.5$ (dashed line), $g_{YB} = -0.4$ (dotted line). The gray area denotes the experimental 1σ interval

1.5 TeV and $g_B = 0.2$. Then we plot $Br(\bar{B} \to X_s\gamma)$ and $Br(B_s^0 \to \mu^+\mu^-)$ varying with $\tan\beta'$ in Fig. 9, for $g_{YB} = -0.6$ (solid line), $g_{YB} = -0.5$ (dashed line), $g_{YB} = -0.4$ (dotted line), respectively. Considering the constraint from concrete Higgs boson mass, the allowed range of $\tan\beta'$ is $1.12 < \tan\beta' < 1.5$. The gray area denotes the experimental 1σ bounds. The picture shows that the numerical results of $Br(\bar{B} \to X_s\gamma)$ depend on g_{YB} or $\tan\beta'$ weakly in our chosen parameter space. Meanwhile, $Br(B_s^0 \to \mu^+\mu^-)$ depends on $\tan\beta'$ more acutely when $|g_{YB}|$ is lager, and can exceed the experimental 1σ upper bound easily with the increasing of $\tan\beta'$ when $g_{YB} = -0.6$, which indicates that the effect of $\tan\beta'$ to the process is influenced by the strength of gauge kinetic mixing strongly. $\tan\beta'$ affects $Br(B_s^0 \to \mu^+\mu^-)$ mainly through the new definition of up type squarks, new scalar and pseudoscalar Higgs bosons. In addition, $Br(B_s^0 \to \mu^+\mu^-)$ increases with the increasing of $|g_{YB}|$ and depend on g_{YB} acutely when $\tan\beta'$ is large.

Then we take $\tan\beta' = 1.2$, and plot $Br(\bar{B} \to X_s\gamma)$ and $Br(B_s^0 \to \mu^+\mu^-)$ varying with g_B in Fig. 10, for $g_{YB} = -0.6$ (solid line), $g_{YB} = -0.5$ (dashed line), $g_{YB} = -0.4$ (dotted line), respectively. Considering the constraints from the concrete Higgs boson mass, the allowed range of g_B is $0.13 < g_B < 0.7$. The gray area denotes the experi-

mental 1σ bounds. It can be noted that g_B and g_{YB} do not affect $Br(\bar{B} \to X_s\gamma)$ obviously. And $Br(B_s^0 \to \mu^+\mu^-)$ can exceed the experimental 1σ upper bound easily when g_B is small and $|g_{YB}|$ is large. In addition, with the decreasing of $|g_{YB}|$, $Br(B_s^0 \to \mu^+\mu^-)$ depends on g_B negligibly, which indicates that the effect of g_B to the process is influenced by the strength of gauge kinetic mixing strongly. g_B and g_{YB} affect $Br(B_s^0 \to \mu^+\mu^-)$ mainly in two ways. Firstly, g_B and g_{YB} affect the up type squark masses and the corresponding rotation matrix, which appears in the couplings involve the up type squarks. Secondly, they affect the process $B_s^0 \to \mu^+\mu^-$ by influencing the new contributions from Z' gauge boson, new scalar and pseudoscalar Higgs bosons in Fig. 4.

5 Summary

Rare B-meson decays offer high sensitivity to new physics beyond SM. In this work, we study the two loop electroweak corrections to the branching ratios $Br(\bar{B} \to X_s\gamma)$ and $Br(B_s^0 \to \mu^+\mu^-)$ in the framework of the B-LSSM under a minimal flavor violating assumption. Considering the constraint from the observed Higgs signal and updated experimental data, the numerical analyses indicate that the corrections from two loop diagrams to the process $\bar{B} \to X_s\gamma$ can reach around 3%, which produces a more precise prediction on the process $\bar{B} \to X_s\gamma$. Nevertheless, the corrections from two loop diagrams to the process $B_s^0 \to \mu^+\mu^-$ are negligible, compared with the one loop corrections. Meanwhile, the new physics can fit the experimental data for the rare decay $\bar{B} \to X_s\gamma$ and $B_s^0 \to \mu^+\mu^-$, and also further constrain the parameter space of the model. Under our assumption on parameters of the considered model, A_t, $\tan\beta$, $M_{H^\pm}$ affect the theoretical predictions on $Br(\bar{B} \to X_s\gamma)$ and $Br(B_s^0 \to \mu^+\mu^-)$ obviously. And when $\tan\beta$ is large, A_t is limited strongly by the experimental data for $Br(B_s^0 \to \mu^+\mu^-)$. In addition, $\tan\beta'$, g_{YB} and g_B can also affect theoretical prediction on $Br(B_s^0 \to \mu^+\mu^-)$ obviously.

Acknowledgements The work has been supported by the National Natural Science Foundation of China (NNSFC) with Grants No. 11535002, No. 11705045, and No. 11647120, Natural Science Foundation of Hebei province with Grants No. A2016201010 and No. A2016201069, Foundation of Department of Education of Liaoning province with Grant No. 2016TSPY10, Youth Foundation of the University of Science and Technology Liaoning with Grant No. 2016QN11, Hebei Key Lab of Optic-Eletronic Information and Materials, and the Midwest Universities Comprehensive Strength Promotion project.

Funded by SCOAP[3].

Appendix A: The Wilson coefficients corresponding to Fig. 3

The Wilson coefficients corresponding to Fig. 3 can be written as

$$
\begin{aligned}
C_7^{\gamma'\text{-exchange}}(\mu_{EW}) = {} & \frac{s_W^2 x_t C^L_{H_j^- \bar{s}t} C^L_{H_j^- b\bar{t}}}{-2(4\pi)^2 V_{ts}^* V_{tb} x_b}\Bigg[-\frac{\partial^2\varphi}{\partial x_1\partial x_3} \\
& -(x_t + x_{H^\pm})\frac{\partial^3\varphi}{\partial x_1\partial x_2\partial x_3} \\
& -3\frac{\partial^2\varphi}{\partial x_1\partial x_2} + \frac{1}{x_2} + x_{H^\pm}\frac{\partial^3\varphi}{\partial x_1\partial x_1\partial x_2} \\
& + x_t\frac{\partial^3\varphi}{\partial x_1\partial x_2\partial x_2} + \frac{1}{x_2} + 6\frac{\partial\Phi}{\partial x_1} \\
& + 2(x_t + x_{H^\pm})\frac{\partial^2\Phi}{\partial x_1\partial x_3} \\
& + (x_t + x_{H^\pm})^2\frac{\partial^3\Phi}{\partial x_1\partial x_2\partial x_3} \\
& + (8x_t + 8x_{H^\pm}) \\
& \frac{\partial^2\Phi}{\partial x_1\partial x_2} + 2x_{H^\pm}^2\frac{\partial^3\Phi}{\partial x_1\partial x_1\partial x_2} \\
& + 2(x_t^2 + x_t x_{H^\pm})\frac{\partial^3\Phi}{\partial x_1\partial x_2\partial x_2}\Bigg] \\
& \times (x_{H^\pm}, x_t, x_{H^\pm}), \\
C_8^{\gamma\text{-exchange}}(\mu_{EW}) = {} & \frac{s_W^2 x_t C^L_{H_j^- \bar{s}t} C^L_{H_j^- b\bar{t}}}{-3(4\pi)^2 V_{ts}^* V_{tb} x_b}\Bigg[-\frac{\partial^2\varphi}{\partial x_1\partial x_2} \\
& + x_t\frac{\partial^3\varphi}{\partial x_1\partial x_2\partial x_2} + 2\frac{\partial\Phi}{\partial x_1} \\
& + 2(2x_t + x_{H^\pm})\frac{\partial^2\Phi}{\partial x_1\partial x_2} \\
& + 2(x_t^2 + x_t x_{H^\pm})\frac{\partial^3\Phi}{\partial x_1\partial x_2\partial x_2}\Bigg] \\
& \times (x_{H^\pm}, x_t, x_{H^\pm}),
\end{aligned}
\tag{A1}
$$

where

$$
\begin{aligned}
\varphi(x_1, x_2, x_3) = {} & x_3\Bigg[\frac{x_1\ln^2 x_1 - x_2\ln^2 x_2}{x_1 - x_2} \\
& + \frac{2\ln(x_3 - x_1)(x_1\ln x_1 - x_2\ln x_2)}{x_1 - x_2} \\
& + 2 - \ln x_3 + \ln^2 x_3\Bigg], \\
\Phi(x_1, x_2, x_3) = {} & \frac{1}{x_1 - x_2}\Bigg[-2x_1\ln^2 x_1 + 2x_2\ln^2 x_2 \\
& + x_1\ln^2\frac{x_1}{x_3} - x_2\ln^2\frac{x_2}{x_3} \\
& + 2(x_1 - x_3)L_{i_2}\left(1 - \frac{x_1}{x_3}\right) \\
& - 2(x_2 - x_3)L_{i_2}\left(1 - \frac{x_2}{x_3}\right)\Bigg].
\end{aligned}
\tag{A2}
$$

The corrections to $Br(\bar{B} \to X_s\gamma)$ can only reach 0.1% in our chosen parameter space.

Appendix B: The Wilson coefficients of the process $\bar{B} \to X_s\gamma$

The one loop Wilson coefficients corresponding to $b \to s\gamma$ can be written as

$$
\begin{aligned}
C_{7,NP}^{(1)}(\mu_{EW}) = & \sum_{H_i^-,u_j} \frac{s_W^2}{2e^2V_{ts}^*V_{tb}} \left\{ \frac{1}{2} C^R_{H_i^-\bar{s}u_j} C^L_{H_i^- b\bar{u}_j} \right. \\
& \left[-I_3(x_{u_j}, x_{H_i^-}) + I_4(x_{u_j}, x_{H_i^-}) \right] \\
& + \frac{m_{u_j}}{m_b} C^L_{H_i^-\bar{s}u_j} C^L_{H_i^- b\bar{u}_j} \left[-I_1(x_{u_j}, x_{H_i^-}) \right. \\
& \left. \left. + I_3(x_{u_j}, x_{H_i^-}) \right] \right\}, \\
C_{7,NP}^{(2)}(\mu_{EW}) = & \sum_{H_j^-,u_i} \frac{s_W^2}{3e^2V_{ts}^*V_{tb}} \left\{ \frac{1}{2} C^R_{H_j^-\bar{s}u_i} C^L_{H_j^- b\bar{u}_i} \right. \\
& \left[-I_1(x_{u_i}, x_{H_j^-}) + 2I_3(x_{u_i}, x_{H_j^-}) \right. \\
& \left. - I_4(x_{u_i}, x_{H_j^-}) \right] \\
& + \frac{m_{u_i}}{m_b} C^L_{H_j^-\bar{s}u_i} C^L_{H_j^- b\bar{u}_i} \left[I_1(x_{u_i}, x_{H_j^-}) \right. \\
& \left. \left. - I_2(x_{u_i}, x_{H_j^-}) - I_3(x_{u_i}, x_{H_j^-}) \right] \right\}, \\
C_{7,NP}^{(3)}(\mu_{EW}) = & \sum_{U_i^+,\chi_j^-} \frac{s_W^2}{3e^2V_{ts}^*V_{tb}} \left\{ \frac{1}{2} C^R_{U_i^+\bar{s}\chi_j^-} C^L_{U_i^+ b\bar{\chi}_j^-} \right. \\
& \left[-I_3(x_{\chi_j^-}, x_{U_i^+}) + I_4(x_{\chi_j^-}, x_{U_i^+}) \right] \\
& + \frac{m_{\chi_j^-}}{m_b} C^L_{U_i^+\bar{s}\chi_j^-} C^L_{U_i^+ b\bar{\chi}_j^-} \left[-I_1(x_{\chi_j^-}, x_{U_i^+}) \right. \\
& \left. \left. + I_3(x_{\chi_j^-}, x_{U_i^+}) \right] \right\}, \\
C_{7,NP}^{(4)}(\mu_{EW}) = & \sum_{U_j^+,\chi_i^-} \frac{s_W^2}{2e^2V_{ts}^*V_{tb}} \left\{ \frac{1}{2} C^R_{U_i^+\bar{s}\chi_i^-} C^L_{U_j^+ b\bar{\chi}_i^-} \right. \\
& \left[-I_1(x_{\chi_i^-}, x_{U_j^+}) + 2I_2(x_{\chi_i^-}, x_{U_j^+}) \right. \\
& \left. - I_4(x_{\chi_i^-}, x_{U_j^+}) \right] \\
& + \frac{m_{\chi_i^-}}{m_b} C^L_{U_j^+\bar{s}\chi_i^-} C^L_{U_j^+ b\bar{\chi}_i^-} \left[I_1(x_{\chi_i^-}, x_{U_j^+}) \right. \\
& \left. \left. - I_2(x_{\chi_i^-}, x_{U_j^+}) - I_3(x_{\chi_i^-}, x_{U_j^+}) \right] \right\}, \\
C_7^{\prime NP(a)}(\mu_{EW}) = & C_7^{\prime NP(a)}(\mu_{EW})(L \leftrightarrow R), (a = 1, 2, 3, 4),
\end{aligned}
\tag{B1}
$$

where S dentes CP-even and CP-odd Higgs, $C_{abc}^{L,R}$ denotes the constant parts of the interaction vertex about abc, which can be got through SARAH, and a, b, c denote the interactional particles. L and R in superscript denote the left-hand part and right-hand part. Denoting $x_i = \frac{m_i^2}{m_W^2}$, the concrete expressions for $I_k (k = 1, \ldots, 4)$ can be given as:

$$
\begin{aligned}
I_1(x_1, x_2) = & \frac{1 + \ln x_2}{(x_2 - x_1)} + \frac{x_1 \ln x_1 - x_2 \ln x_2}{(x_2 - x_1)^2}, \\
I_2(x_1, x_2) = & -\frac{1 + \ln x_1}{(x_2 - x_1)} - \frac{x_1 \ln x_1 - x_2 \ln x_2}{(x_2 - x_1)^2}, \\
I_3(x_1, x_2) = & \frac{1}{2} \left[\frac{3 + 2\ln x_2}{(x_2 - x_1)} - \frac{2x_2 + 4x_2 \ln x_2}{(x_2 - x_1)^2} \right. \\
& \left. - \frac{2x_1^2 \ln x_1}{(x_2 - x_1)^3} + \frac{2x_2^2 \ln x_2}{(x_2 - x_1)^3} \right], \\
I_4(x_1, x_2) = & \frac{1}{4} \left[\frac{11 + 6\ln x_2}{(x_2 - x_1)} - \frac{15x_2 + 18x_2 \ln x_2}{(x_2 - x_1)^2} \right. \\
& \left. + \frac{6x_2^2 + 18x_2^2 \ln x_2}{(x_2 - x_1)^3} + \frac{6x_1^3 \ln x_1 - 6x_2^3 \ln x_2}{(x_2 - x_1)^4} \right].
\end{aligned}
\tag{B2}
$$

Assuming $m_{\chi_i^\pm},\ m_{\chi_j^0} \gg m_W$, then the two loop Wilson coefficients corresponding to $b \to s\gamma$ can be simplified as

$$
\begin{aligned}
C_{7,NP}^{WW}(\mu_{EW}) = & \sum_{\chi_i^\pm,\chi_j^0} \frac{-1}{8\pi^2} \left\{ \left(|C^L_{W^-\bar{\chi}_j^0\chi_i^+}|^2 + |C^R_{W^-\bar{\chi}_j^0\chi_i^+}|^2 \right) \right. \\
& \times \left[P\left(\frac{1}{8}, \frac{1}{4}, \frac{-1}{48}, \frac{-1}{144}, 1, x_t \right) \right. \\
& \left. + \frac{2}{3} P\left(\frac{-11}{12}, \frac{-29}{72}, \frac{-1}{12}, \frac{1}{144}, 1, x_t \right) \right] \\
& + \left(C^R_{W^-\bar{\chi}_j^0\chi_i^+} C^{L*}_{W^-\bar{\chi}_j^0\chi_i^+} + C^L_{W^-\bar{\chi}_j^0\chi_i^+} \right. \\
& \left. C^{R*}_{W^-\bar{\chi}_j^0\chi_i^+} \right) \left[P\left(\frac{1}{16}, \frac{1}{4}, \frac{-1}{16}, \frac{1}{144}, 1, x_t \right) \right. \\
& \left. + \frac{2}{3} P\left(\frac{-11}{12}, \frac{-29}{72}, \frac{-1}{12}, \frac{1}{144}, 1, x_t \right) \right] \\
& + \frac{1}{8} \left(C^L_{W^-\bar{\chi}_j^0\chi_i^+} C^{R*}_{W^-\bar{\chi}_j^0\chi_i^+} \right. \\
& \left. \left. - C^R_{W^-\bar{\chi}_j^0\chi_i^+} C^{L*}_{W^-\bar{\chi}_j^0\chi_i^+} \right) \frac{\partial^2 \rho_{2,1}}{\partial x_1^2}(x_W, x_t) \right\}, \\
C_{8,NP}^{WW}(\mu_{EW}) = & \sum_{\chi_i^\pm,\chi_j^0} \frac{-3}{8\pi^2} \left\{ \left(|C^L_{W^-\bar{\chi}_j^0\chi_i^+}|^2 + |C^R_{W^-\bar{\chi}_j^0\chi_i^+}|^2 \right) \right. \\
& \times P\left(\frac{-11}{12}, \frac{-29}{72}, \frac{-1}{12}, \frac{1}{144}, 1, x_t \right) \\
& + \left(C^R_{W^-\bar{\chi}_j^0\chi_i^+} C^{L*}_{W^-\bar{\chi}_j^0\chi_i^+} \right.
\end{aligned}
$$

$$
\begin{aligned}
&+C^{L}_{W^-\bar{\chi}^0_j\chi_i^+}C^{R*}_{W^-\bar{\chi}^0_j\chi_i^+}\Big)\\
&\times P\left(\frac{-1}{12},\frac{-5}{24},\frac{1}{12},\frac{-1}{144},1,x_t\right)\\
&+\Big(C^{R}_{W^-\bar{\chi}^0_j\chi_i^+}C^{L*}_{W^-\bar{\chi}^0_j\chi_i^+}\\
&-C^{L}_{W^-\bar{\chi}^0_j\chi_i^+}C^{R*}_{W^-\bar{\chi}^0_j\chi_i^+}\Big)\\
&\times P\left(\frac{1}{16},\frac{7}{24},0,0,1,x_t\right)\Big\},\\
C^{WH}_{7,NP}(\mu_{EW}) &= \sum_{\chi_i^\pm,\chi_j^0}\frac{C^{L}_{H^-\bar{d}u}m_W^2}{4\sqrt{2}\pi^2 m_s m_F V^*_{ts}}\\
&\times\Big\{\Big[\Re\Big(C^{L}_{H^-\bar{\chi}^0_j\chi_i^+}C^{L}_{W^-\bar{\chi}^0_j\chi_i^+}\\
&+C^{R}_{H^-\bar{\chi}^0_j\chi_i^+}C^{R}_{W^-\bar{\chi}^0_j\chi_i^+}\Big)\\
&-i\Im\Big(C^{L}_{H^-\bar{\chi}^0_j\chi_i^+}C^{L}_{W^-\bar{\chi}^0_j\chi_i^+}\\
&+C^{R}_{H^-\bar{\chi}^0_j\chi_i^+}C^{R}_{W^-\bar{\chi}^0_j\chi_i^+}\Big)\Big]\Big(\frac{21}{64}-\frac{5}{288}\\
&+\frac{5}{24}J(m_W^2,M^2_{H^\pm},m_t^2)\Big)\\
&+\Big[\Re\Big(C^{L}_{H^-\bar{\chi}^0_j\chi_i^+}C^{R}_{W^-\bar{\chi}^0_j\chi_i^+}\\
&+C^{R}_{H^-\bar{\chi}^0_j\chi_i^+}C^{L}_{W^-\bar{\chi}^0_j\chi_i^+}\Big)\\
&-i\Im\Big(C^{L}_{H^-\bar{\chi}^0_j\chi_i^+}C^{R}_{W^-\bar{\chi}^0_j\chi_i^+}\\
&+C^{R}_{H^-\bar{\chi}^0_j\chi_i^+}C^{L}_{W^-\bar{\chi}^0_j\chi_i^+}\Big)\Big]\Big(\frac{-1}{144}-\frac{1}{24}J(m_W^2,\\
&M^2_{H^\pm},m_t^2)\Big)-\Big[\Re\Big(C^{L}_{H^-\bar{\chi}^0_j\chi_i^+}C^{L}_{W^-\bar{\chi}^0_j\chi_i^+}\\
&-C^{R}_{H^-\bar{\chi}^0_j\chi_i^+}C^{R}_{W^-\bar{\chi}^0_j\chi_i^+}\Big)\\
&-i\Im\Big(C^{L}_{H^-\bar{\chi}^0_j\chi_i^+}C^{L}_{W^-\bar{\chi}^0_j\chi_i^+}\\
&-C^{R}_{H^-\bar{\chi}^0_j\chi_i^+}C^{R}_{W^-\bar{\chi}^0_j\chi_i^+}\Big)\Big]\Big(\frac{16}{144}\\
&+\frac{1}{6}J(m_W^2,M^2_{H^\pm},m_t^2)\Big)\\
&-\Big[\Re\Big(C^{L}_{H^-\bar{\chi}^0_j\chi_i^+}C^{R}_{W^-\bar{\chi}^0_j\chi_i^+}\\
&-C^{R}_{H^-\bar{\chi}^0_j\chi_i^+}C^{L}_{W^-\bar{\chi}^0_j\chi_i^+}\Big)\\
&-i\Im\Big(C^{L}_{H^-\bar{\chi}^0_j\chi_i^+}C^{R}_{W^-\bar{\chi}^0_j\chi_i^+}\\
&-C^{R}_{H^-\bar{\chi}^0_j\chi_i^+}C^{L}_{W^-\bar{\chi}^0_j\chi_i^+}\Big)\Big]\Big(\frac{1}{72}+\frac{1}{12}J(m_W^2,\\
&M^2_{H^\pm},m_t^2)\Big)\Big\},\\
C^{WH}_{8,NP}(\mu_{EW}) &= \sum_{\chi_i^\pm,\chi_j^0}\frac{C^{L}_{H^-\bar{d}u}m_W^2}{4\sqrt{2}\pi^2 m_s m_F V^*_{ts}}\Big\{\Big[\Re\Big(C^{L}_{H^-\bar{\chi}^0_j\chi_i^+}\\
&\times C^{L}_{W^-\bar{\chi}^0_j\chi_i^+}+C^{R}_{H^-\bar{\chi}^0_j\chi_i^+}C^{R}_{W^-\bar{\chi}^0_j\chi_i^+}\Big)\\
&-i\Im\Big(C^{L}_{H^-\bar{\chi}^0_j\chi_i^+}C^{L}_{W^-\bar{\chi}^0_j\chi_i^+}\\
&+C^{R}_{H^-\bar{\chi}^0_j\chi_i^+}C^{R}_{W^-\bar{\chi}^0_j\chi_i^+}\Big)\Big]\\
&\times\Big(\frac{-1}{8\sqrt{2}}J(m_W^2,M^2_{H^\pm},m_t^2)\Big)\\
&+\Big[\Re\Big(C^{L}_{H^-\bar{\chi}^0_j\chi_i^+}C^{R}_{W^-\bar{\chi}^0_j\chi_i^+}\\
&+C^{R}_{H^-\bar{\chi}^0_j\chi_i^+}C^{L}_{W^-\bar{\chi}^0_j\chi_i^+}\Big)\\
&+i\Im\Big(C^{L}_{H^-\bar{\chi}^0_j\chi_i^+}C^{R}_{W^-\bar{\chi}^0_j\chi_i^+}\\
&+C^{R}_{H^-\bar{\chi}^0_j\chi_i^+}C^{L}_{W^-\bar{\chi}^0_j\chi_i^+}\Big)\Big]\\
&\times\Big(\frac{-1}{8\sqrt{2}}J(m_W^2,M^2_{H^\pm},m_t^2)\Big)\\
&+\Big[\Re\Big(C^{L}_{H^-\bar{\chi}^0_j\chi_i^+}C^{L}_{W^-\bar{\chi}^0_j\chi_i^+}\\
&-C^{R}_{H^-\bar{\chi}^0_j\chi_i^+}C^{R}_{W^-\bar{\chi}^0_j\chi_i^+}\Big)\\
&-i\Im\Big(C^{L}_{H^-\bar{\chi}^0_j\chi_i^+}C^{L}_{W^-\bar{\chi}^0_j\chi_i^+}\\
&-C^{R}_{H^-\bar{\chi}^0_j\chi_i^+}C^{R}_{W^-\bar{\chi}^0_j\chi_i^+}\Big)\Big]\\
&\times\Big(\frac{-1}{4\sqrt{2}}J(m_W^2,M^2_{H^\pm},m_t^2)\Big)\\
&+\Big[\Re\Big(C^{L}_{H^-\bar{\chi}^0_j\chi_i^+}C^{R}_{W^-\bar{\chi}^0_j\chi_i^+}\\
&+C^{R}_{H^-\bar{\chi}^0_j\chi_i^+}C^{L}_{W^-\bar{\chi}^0_j\chi_i^+}\Big)\\
&+i\Im\Big(C^{L}_{H^-\bar{\chi}^0_j\chi_i^+}C^{R}_{W^-\bar{\chi}^0_j\chi_i^+}\\
&+C^{R}_{H^-\bar{\chi}^0_j\chi_i^+}C^{L}_{W^-\bar{\chi}^0_j\chi_i^+}\Big)\Big]\\
&\times\Big(\frac{1}{4\sqrt{2}}J(m_W^2,M^2_{H^\pm},m_t^2)\Big)\Big\},
\end{aligned}
\tag{B3}
$$

where m_F runs all $m_{\chi_i^\pm}$, $m_{\chi_j^0}$, and

$$\begin{aligned}
&\rho_{i,j}(x_1,x_2)=\frac{x_1^i\ln^j x_1-x_2^i\ln^j x_2}{x_1-x_2},\\
&P(y_1,y_2,y_3,y_4,x_1,x_2)=y_1\frac{\partial\rho_{1,1}(x_1,x_2)}{\partial x_1}\\
&\quad+y_2\frac{\partial^2\rho_{2,1}(x_1,x_2)}{\partial x_1^2}\\
&\quad+y_3\frac{\partial^3\rho_{3,1}(x_1,x_2)}{\partial x_1^3}\\
&\quad+y_4\frac{\partial^4\rho_{4,1}(x_1,x_2)}{\partial x_1^4},\\
&J(x_1,x_2,x_3)=\ln m_F^2\\
&\quad-\frac{\rho_{2,1}(x_1,x_3)-\rho_{2,2}(x_2,x_3)}{x_1^2-x_2^2}
\end{aligned}\tag{B4}$$

Appendix C: The Wilson coefficients of the process $B_s^0\to\mu^+\mu^-$

The Wilson coefficients corresponding to $b\to s\mu^+\mu^-$ can be written as

$$\begin{aligned}
C_{S,NP}^{(1)}(\mu_{\rm EW})=&\sum_{\tilde{U}_i,\chi_j^-,\chi_k^-,S=h_l,A_l}\frac{C_{\mu^-S\mu^+}^L+C_{\mu^-S\mu^+}^R}{2\left(m_b^2-m_S^2\right)}\\
&\times\Bigg[C_{\tilde{U}_i\bar{s}\chi_j^-}^R C_{\bar{\chi}_j^-S\chi_k^-}^L C_{\bar{\chi}_k^-s\tilde{U}_i}^R\\
&\times G_2\left(x_{\tilde{U}_i},x_{\chi_j^\pm},x_{\chi_k^\pm}\right)+M_{\chi_j^\pm}M_{\chi_k^\pm}\\
&\times C_{\tilde{U}_i\bar{s}\chi_j^-}^R C_{\bar{\chi}_j^-S\chi_k^-}^R C_{\bar{\chi}_k^-s\tilde{U}_i}^R\\
&\times G_1\left(x_{\tilde{U}_i},x_{\chi_j^\pm},x_{\chi_k^\pm}\right)\Bigg]\\
&+\sum_{H_i^-,u_j,u_k,S=h_l,A_l}\frac{C_{\mu^-S\mu^+}^L+C_{\mu^-S\mu^+}^R}{2\left(m_b^2-m_S^2\right)}\\
&\times\Bigg[C_{H_i^-\bar{s}u_j}^R C_{\bar{u}_jSu_k}^L C_{\bar{u}_kbH_i^-}^R\\
&\times G_2\left(x_{\tilde{H}_i^\pm},x_{u_j},x_{u_k}\right)+m_{u_j}m_{u_k}\\
&\times C_{H_i^-\bar{s}u_j}^R C_{\bar{u}_jSu_k}^R C_{\bar{u}_kbH_i^-}^R\\
&\times G_1\left(x_{\tilde{H}_i^\pm},x_{u_j},x_{u_k}\right)\Bigg],\\
C_{P,NP}^{(1)}(\mu_{\rm EW})=&\sum_{\tilde{U}_i,\chi_j^-,\chi_k^-,S=h_l,A_l}\frac{-C_{\mu^-S\mu^+}^L+C_{\mu^-S\mu^+}^R}{2\left(m_b^2-m_S^2\right)}\\
&\times\Bigg[C_{\tilde{U}_i\bar{s}\chi_j^-}^R C_{\bar{\chi}_j^-S\chi_k^-}^L C_{\bar{\chi}_k^-s\tilde{U}_i}^R\\
&\times G_2\left(x_{\tilde{U}_i},x_{\chi_j^\pm},x_{\chi_k^\pm}\right)\\
&+M_{\chi_j^\pm}M_{\chi_k^\pm}C_{\tilde{U}_i\bar{s}\chi_j^-}^R C_{\bar{\chi}_j^-S\chi_k^-}^R C_{\bar{\chi}_k^-s\tilde{U}_i}^R\\
&\times G_1\left(x_{\tilde{U}_i},x_{\chi_j^\pm},x_{\chi_k^\pm}\right)\Bigg]\\
&+\sum_{H_i^-,u_j,u_k,S=h_l,A_l}\frac{-C_{\mu^-S\mu^+}^L+C_{\mu^-S\mu^+}^R}{2\left(m_b^2-m_S^2\right)}\\
&\times\Bigg[C_{H_i^-\bar{s}u_j}^R C_{\bar{u}_jSu_k}^L C_{\bar{u}_kbH_i^-}^R\\
&\times G_2\left(x_{\tilde{H}_i^\pm},x_{u_j},x_{u_k}\right)\\
&+m_{u_j}m_{u_k}C_{H_i^-\bar{s}u_j}^R C_{\bar{u}_jSu_k}^R\\
&\times C_{\bar{u}_kbH_i^-}^R G_1\left(x_{\tilde{H}_i^\pm},x_{u_j},x_{u_k}\right)\Bigg],
\end{aligned}\tag{C1}$$

$$\begin{aligned}
C_{S,NP}^{(2)}(\mu_{\rm EW})=&\sum_{u_i,H_j^\pm,H_k^\pm,S=h_l,A_l}\frac{1}{2\left(m_b^2-m_S^2\right)}\\
&\times m_{u_i}C_{\bar{s}u_iH_j^\pm}^R\\
&\times C_{\bar{u}_ibH_k^\pm}^R C_{SH_j^\pm H_k^\pm}G_1\left(x_{u_i},x_{H_j^\pm},x_{H_k^\pm}\right)\\
&\times\left(C_{\mu^-S\mu^+}^L+C_{\mu^-S\mu^+}^R\right)\\
&+\sum_{\chi_i^\pm,\tilde{U}_j,\tilde{U}_k,S=h_l,A_l}\frac{1}{2\left(m_b^2-m_S^2\right)}\\
&\times m_{\chi_i^\pm}C_{\bar{s}\chi_i^\pm\tilde{U}_j}^R\\
&\times C_{\bar{\chi}_i^\pm b\tilde{U}_k}^R C_{S\tilde{U}_j\tilde{U}_k}G_1\left(x_{\chi_i^\pm},x_{\tilde{U}_j},x_{\tilde{U}_k}\right)\\
&\times\left(C_{\mu^-S\mu^+}^L+C_{\mu^-S\mu^+}^R\right),\\
C_{p,NP}^{(2)}(\mu_{\rm EW})=&\sum_{u_i,H_j^\pm,H_k^\pm,S=h_l,A_l}\frac{1}{2\left(m_b^2-m_S^2\right)}m_{u_i}C_{\bar{s}u_iH_j^\pm}^R\\
&\times C_{\bar{u}_ibH_k^\pm}^R C_{SH_j^\pm H_k^\pm}G_1\left(x_{u_i},x_{H_j^\pm},x_{H_k^\pm}\right)\\
&\times\left(-C_{\mu^-S\mu^+}^L+C_{\mu^-S\mu^+}^R\right)\\
&+\sum_{\chi_i^\pm,\tilde{U}_j,\tilde{U}_k,S=h_l,A_l}\frac{1}{2\left(m_b^2-m_S^2\right)}\\
&\times m_{\chi_i^\pm}C_{\bar{s}\chi_i^\pm\tilde{U}_j}^R\\
&\times C_{\bar{\chi}_i^\pm b\tilde{U}_k}^R C_{S\tilde{U}_j\tilde{U}_k}G_1\left(x_{\chi_i^\pm},x_{\tilde{U}_j},x_{\tilde{U}_k}\right)\\
&\times\left(-C_{\mu^-S\mu^+}^L+C_{\mu^-S\mu^+}^R\right),
\end{aligned}\tag{C2}$$

$$\begin{aligned}
C_{S,NP}^{(3)}(\mu_{\rm EW})=&\sum_{u_i,H_k^\pm,S=h_l,A_l}\frac{-C_{W^\pm SH_k^\pm}}{2\left(m_b^2-m_S^2\right)}\Big[C_{\bar{s}W^\pm u_i}^L\\
&\times C_{\bar{u}_iH_k^\pm b}^R G_2\left(x_{u_i},1,x_{H_k^\pm}\right)\\
&-2m_bm_{u_i}C_{\bar{s}W^\pm u_i}^L\\
&\times C_{\bar{u}_iH_k^\pm b}^L G_1\left(x_{u_i},1,x_{H_k^\pm}\right)\Big]\\
&\times\left(C_{\mu^-S\mu^+}^L+C_{\mu^-S\mu^+}^R\right),
\end{aligned}$$

$$
\begin{aligned}
C^{(3)}_{P,NP}\left(\mu_{\rm EW}\right) = & \sum_{u_i,H^\pm_k,S=h_l,A_l} \frac{-C_{W^\pm S H^\pm_k}}{2\left(m_b^2-m_S^2\right)}\Big[C^L_{\bar{s}W^\pm u_i} \\
& \times C^R_{\bar{u}_i H^\pm_k b} G_2\left(x_{u_i},1,x_{H^\pm_k}\right) \\
& -2m_b m_{u_i} C^L_{\bar{s}W^\pm u_i} \\
& \times C^L_{\bar{u}_i H^\pm_k b} G_1\left(x_{u_i},1,x_{H^\pm_k}\right)\Big] \\
& \times \left(-C^L_{\mu^- S\mu^+} + C^R_{\mu^- S\mu^+}\right), \qquad \text{(C3)} \\
C^{(4)}_{S,NP}\left(\mu_{\rm EW}\right) = & \sum_{u_i,H^\pm_j,S=h_l,A_l} \frac{-C_{W^\pm S H^\pm_j}}{2\left(m_b^2-m_S^2\right)} C^R_{\bar{s}H^\pm_j u_i} \\
& \times C^R_{\bar{u}_i W^\pm b} G_2\left(x_{u_i},x_{H^\pm_j},1\right) \\
& \times \left(C^L_{\mu^- S\mu^+} + C^R_{\mu^- S\mu^+}\right), \\
C^{(4)}_{S,NP}\left(\mu_{\rm EW}\right) = & \sum_{u_i,H^\pm_j,S=h_l,A_l} \frac{-C_{W^\pm S H^\pm_j}}{2\left(m_b^2-m_S^2\right)} C^R_{\bar{s}H^\pm_j u_i} \\
& \times C^R_{\bar{u}_i W^\pm b} G_2\left(x_{u_i},x_{H^\pm_j},1\right) \\
& \times \left(-C^L_{\mu^- S\mu^+} + C^R_{\mu^- S\mu^+}\right), \qquad \text{(C4)} \\
C^{(5)}_{9,NP}\left(\mu_{\rm EW}\right) = & \sum_{\tilde{U}_i,\chi^-_j,\chi^-_k,V} \frac{C^L_{\mu^- V\mu^+} + C^R_{\mu^- V\mu^+}}{-2\left(m_b^2-m_V^2\right)} \\
& \times \Big[-\frac{1}{2} C^R_{\tilde{U}_i \bar{s}\chi^-_j} C^R_{\bar{\chi}^-_j V\chi^-_k} \\
& \times C^L_{\bar{\chi}^-_k s\tilde{U}_i} G_2\left(x_{\tilde{U}_i},x_{\chi^\pm_j},x_{\chi^\pm_k}\right) \\
& + M_{\chi^\pm_j} M_{\chi^\pm_k} C^R_{\tilde{U}_i \bar{s}\chi^-_j} C^L_{\bar{\chi}^-_j V\chi^-_k} \\
& \times C^L_{\bar{\chi}^-_k s\tilde{U}_i} G_1\left(x_{\tilde{U}_i},x_{\chi^\pm_j},x_{\chi^\pm_k}\right)\Big] \\
& + \sum_{\tilde{H}^\pm_i,u_j,u_k,V} \frac{-C^L_{\mu^- V\mu^+} + C^R_{\mu^- V\mu^+}}{-2\left(m_b^2-m_V^2\right)} \\
& \times \Big[-\frac{1}{2} C^R_{H^\pm_i \bar{s}u_j} C^R_{\bar{u}_j V u_k} C^L_{u_k s H^\pm_i} \\
& \times G_2\left(x_{H^\pm_i},x_{u_j},x_{u_k}\right) \\
& + m_{u_j} m_{u_k} C^R_{H^\pm_i \bar{s}u_j} C^L_{\bar{u}_j V u_k} C^L_{\bar{u}_k s H^\pm_i} \\
& \times G_1\left(x_{H^\pm_i},x_{u_j},x_{u_k}\right)\Big], \\
C^{(5)}_{10,NP}\left(\mu_{\rm EW}\right) = & \sum_{\tilde{U}_i,\chi^-_j,\chi^-_k,V} \frac{-C^L_{\mu^- V\mu^+} + C^R_{\mu^- V\mu^+}}{-2\left(m_b^2-m_V^2\right)} \\
& \times \Big[-\frac{1}{2} C^R_{\tilde{U}_i \bar{s}\chi^-_j} C^R_{\bar{\chi}^-_j V\chi^-_k} \\
& \times C^L_{\bar{\chi}^-_k s\tilde{U}_i} G_2\left(x_{\tilde{U}_i},x_{\chi^\pm_j},x_{\chi^\pm_k}\right) \\
& + M_{\chi^\pm_j} M_{\chi^\pm_k} C^R_{\tilde{U}_i \bar{s}\chi^-_j} C^L_{\bar{\chi}^-_j V\chi^-_k} C^L_{\bar{\chi}^-_k s\tilde{U}_i} \\
& \times G_1\left(x_{\tilde{U}_i},x_{\chi^\pm_j},x_{\chi^\pm_k}\right)\Big] \\
& + \sum_{\tilde{H}^\pm_i,u_j,u_k,V} \frac{-C^L_{\mu^- V\mu^+} + C^R_{\mu^- V\mu^+}}{-2\left(m_b^2-m_V^2\right)} \\
& \times \Big[-\frac{1}{2} C^R_{H^\pm_i \bar{s}u_j} C^R_{\bar{u}_j V u_k} C^L_{u_k s H^\pm_i} \\
& \times G_2\left(x_{H^\pm_i},x_{u_j},x_{u_k}\right) \\
& + m_{u_j} m_{u_k} C^R_{H^\pm_i \bar{s}u_j} C^L_{\bar{u}_j V u_k} C^L_{\bar{u}_k s H^\pm_i} \\
& \times G_1\left(x_{H^\pm_i},x_{u_j},x_{u_k}\right)\Big], \qquad \text{(C5)} \\
C^{(6)}_{9,NP}\left(\mu_{\rm EW}\right) = & \sum_{u_i,H^\pm_j,H^\pm_k,V} \frac{C^L_{\mu^- V\mu^+} + C^R_{\mu^- V\mu^+}}{4\left(m_b^2-m_V^2\right)} \\
& \times C^R_{\bar{s}u_i H^\pm_j} C^L_{\bar{u}_i b H^\pm_k} C_{V H^\pm_j H^\pm_k} \\
& \times G_2\left(x_{u_i},x_{H^\pm_j},x_{H^\pm_k}\right) \\
& + \sum_{\chi^\pm_i,\tilde{U}_j,\tilde{U}_k,V} \frac{C^L_{\mu^- V\mu^+} + C^R_{\mu^- V\mu^+}}{4\left(m_b^2-m_V^2\right)} \\
& \times C^R_{\bar{s}\chi^\pm_i \tilde{U}_j} C^L_{\bar{\chi}^\pm_i b\tilde{U}_k} C_{V\tilde{U}_j\tilde{U}_k} \\
& \times G_2\left(x_{\chi^\pm_i},x_{\tilde{U}_j},x_{\tilde{U}_k}\right), \\
C^{(6)}_{10,NP}\left(\mu_{\rm EW}\right) = & \sum_{u_i,H^\pm_j,H^\pm_k,V} \frac{-C^L_{\mu^- V\mu^+} + C^R_{\mu^- V\mu^+}}{4\left(m_b^2-m_V^2\right)} \\
& \times C^R_{\bar{s}u_i H^\pm_j} C^L_{\bar{u}_i b H^\pm_k} C_{V H^\pm_j H^\pm_k} \\
& \times G_2\left(x_{u_i},x_{H^\pm_j},x_{H^\pm_k}\right) \\
& + \sum_{\chi^\pm_i,\tilde{U}_j,\tilde{U}_k,V} \frac{-C^L_{\mu^- V\mu^+} + C^R_{\mu^- V\mu^+}}{4\left(m_b^2-m_V^2\right)} \\
& \times C^R_{\bar{s}\chi^\pm_i \tilde{U}_j} C^L_{\bar{\chi}^\pm_i b\tilde{U}_k} C_{V\tilde{U}_j\tilde{U}_k} \\
& \times G_2\left(x_{\chi^\pm_i},x_{\tilde{U}_j},x_{\tilde{U}_k}\right), \\
C^{(6)}_{S,NP}\left(\mu_{\rm EW}\right) = & \sum_{u_i,H^\pm_j,H^\pm_k,V} \frac{C^L_{\mu^- V\mu^+} + C^R_{\mu^- V\mu^+}}{-2\left(m_b^2-m_V^2\right)} \\
& \times m_b m_{u_i} C^R_{\bar{s}u_i H^\pm_j} C^R_{\bar{u}_i b H^\pm_k} C_{V H^\pm_j H^\pm_k} \\
& \times G_1\left(x_{u_i},x_{H^\pm_j},x_{H^\pm_k}\right) \\
& + \sum_{\chi^\pm_i,\tilde{U}_j,\tilde{U}_k,V} \frac{C^L_{\mu^- V\mu^+} + C^R_{\mu^- V\mu^+}}{-2\left(m_b^2-m_V^2\right)} \\
& \times m_b m_{\chi^\pm_i} C^R_{\bar{s}\chi^\pm_i \tilde{U}_j} C^R_{\bar{\chi}^\pm_i b\tilde{U}_k} C_{V\tilde{U}_j\tilde{U}_k} \\
& \times G_1\left(x_{\chi^\pm_i},x_{\tilde{U}_j},x_{\tilde{U}_k}\right),
\end{aligned}
$$

$$C^{(6)}_{P,NP}(\mu_{\rm EW}) = \sum_{u_i,H_j^\pm,H_k^\pm,V} \frac{C^L_{\mu^- V\mu^+} - C^R_{\mu^- V\mu^+}}{-2\left(m_b^2 - m_V^2\right)} \times m_b m_{u_i} C^R_{\tilde{s}u_i H_j^\pm} C^R_{\tilde{u}_i b H_k^\pm} C_{V H_j^\pm H_k^\pm} \times G_1\left(x_{u_i}, x_{H_j^\pm}, x_{H_k^\pm}\right) + \sum_{\chi_i^\pm,\tilde{U}_j,\tilde{U}_k,V} \frac{C^L_{\mu^- V\mu^+} - C^R_{\mu^- V\mu^+}}{-2\left(m_b^2 - m_V^2\right)} m_b m_{\chi_i^\pm} \times C^R_{\tilde{s}\chi_i^\pm \tilde{U}_j} C^R_{\tilde{\chi}_i^\pm b \tilde{U}_k} C_{V\tilde{U}_j\tilde{U}_k} \times G_1\left(x_{\chi_i^\pm}, x_{\tilde{U}_j}, x_{\tilde{U}_k}\right), \quad \text{(C6)}$$

$$C^{(7)}_{9,NP}(\mu_{\rm EW}) = \sum_{u_i,H_k^\pm,V} \frac{C^L_{\mu^- V\mu^+} + C^R_{\mu^- V\mu^+}}{2\left(m_b^2 - m_V^2\right)} m_{u_i} C^L_{\tilde{s}u_i W^\pm} \times C^L_{\tilde{u}_i b H_k^\pm} C_{V W^\pm H_k^\pm} G_1\left(x_{u_i}, x_W, x_{H_k^\pm}\right),$$

$$C^{(7)}_{10,NP}(\mu_{\rm EW}) = \sum_{u_i,H_k^\pm,V} \frac{-C^L_{\mu^- V\mu^+} + C^R_{\mu^- V\mu^+}}{2\left(m_b^2 - m_V^2\right)} m_{u_i} C^L_{\tilde{s}u_i W^\pm} \times C^L_{\tilde{u}_i b H_k^\pm} C_{V W^\pm H_k^\pm} G_1\left(x_{u_i}, x_W, x_{H_k^\pm}\right), \quad \text{(C7)}$$

$$C^{(8)}_{9,NP}(\mu_{\rm EW}) = \sum_{u_i,H_j^\pm,V} \frac{C^L_{\mu^- V\mu^+} + C^R_{\mu^- V\mu^+}}{2\left(m_b^2 - m_V^2\right)} \times m_{u_i} C^R_{\tilde{s}u_i H_j^\pm} C^L_{\tilde{u}_i b W^\pm} C_{V W^\pm H_k^\pm} \times G_1\left(x_{u_i}, x_{H_j^\pm}, x_W\right),$$

$$C^{(8)}_{10,NP}(\mu_{\rm EW}) = \sum_{u_i,H_j^\pm,V} \frac{-C^L_{\mu^- V\mu^+} + C^R_{\mu^- V\mu^+}}{2\left(m_b^2 - m_V^2\right)} \times m_{u_i} C^R_{\tilde{s}u_i H_j^\pm} C^L_{\tilde{u}_i b W^\pm} C_{V W^\pm H_k^\pm} \times G_1\left(x_{u_i}, x_{H_j^\pm}, x_W\right), \quad \text{(C8)}$$

$$C^{(9)}_{9,NP}(\mu_{\rm EW}) = \sum_{\tilde{U}_i,\chi_j^\pm,\chi_k^\pm,\tilde{\nu}_l} -\frac{1}{8} C^R_{\tilde{s}\tilde{U}_i\chi_j^\pm} C^L_{\tilde{\chi}_j^\pm \mu^+\tilde{\nu}_l} \times \left(C^L_{\tilde{\mu}^-\tilde{\nu}_l\chi_k^\pm} C^R_{\tilde{\chi}_k^\pm \tilde{U}_i b} + C^R_{\tilde{\mu}^-\tilde{\nu}_l\chi_k^\pm} C^L_{\tilde{\chi}_k^\pm \tilde{U}_i b}\right) \times G_4\left(x_{\tilde{U}_i}, x_{\chi_j^\pm}, x_{\chi_k^\pm}, x_{\tilde{\nu}_l}\right),$$

$$C^{(9)}_{10,NP}(\mu_{\rm EW}) = \sum_{\tilde{U}_i,\chi_j^\pm,\chi_k^\pm,\tilde{\nu}_l} -\frac{1}{8} C^R_{\tilde{s}\tilde{U}_i\chi_j^\pm} C^L_{\tilde{\chi}_j^\pm \mu^+\tilde{\nu}_l} \times \left(C^L_{\tilde{\mu}^-\tilde{\nu}_l\chi_k^\pm} C^R_{\tilde{\chi}_k^\pm \tilde{U}_i b} - C^R_{\tilde{\mu}^-\tilde{\nu}_l\chi_k^\pm} C^L_{\tilde{\chi}_k^\pm \tilde{U}_i b}\right) \times G_4\left(x_{\tilde{U}_i}, x_{\chi_j^\pm}, x_{\chi_k^\pm}, x_{\tilde{\nu}_l}\right),$$

$$C^{(9)}_{S,NP}(\mu_{\rm EW}) = \sum_{\tilde{U}_i,\chi_j^\pm,\chi_k^\pm,\tilde{\nu}_l} -\frac{1}{2} M_{\chi_j^\pm} M_{\chi_k^\pm} \times C^R_{\tilde{s}\tilde{U}_i\chi_j^\pm} C^R_{\tilde{\chi}_j^\pm \mu^+\tilde{\nu}_l} \left(C^L_{\tilde{\mu}^-\tilde{\nu}_l\chi_k^\pm} C^L_{\tilde{\chi}_k^\pm \tilde{U}_i b} + C^R_{\tilde{\mu}^-\tilde{\nu}_l\chi_k^\pm} C^R_{\tilde{\chi}_k^\pm \tilde{U}_i b}\right) G_3\left(x_{\tilde{U}_i}, x_{\chi_j^\pm}, x_{\chi_k^\pm}, x_{\tilde{\nu}_l}\right),$$

$$C^{(9)}_{P,NP}(\mu_{\rm EW}) = \sum_{\tilde{U}_i,\chi_j^\pm,\chi_k^\pm,\tilde{\nu}_l} -\frac{1}{2} M_{\chi_j^\pm} M_{\chi_k^\pm} \times C^R_{\tilde{s}\tilde{U}_i\chi_j^\pm} C^R_{\tilde{\chi}_j^\pm \mu^+\tilde{\nu}_l} \left(-C^L_{\tilde{\mu}^-\tilde{\nu}_l\chi_k^\pm} C^L_{\tilde{\chi}_k^\pm \tilde{U}_i b} + C^R_{\tilde{\mu}^-\tilde{\nu}_l\chi_k^\pm} C^R_{\tilde{\chi}_k^\pm \tilde{U}_i b}\right) G_3\left(x_{\tilde{U}_i}, x_{\chi_j^\pm}, x_{\chi_k^\pm}, x_{\tilde{\nu}_l}\right), \quad \text{(C9)}$$

$$C^{(10)}_{9,NP}(\mu_{\rm EW}) = \sum_{u_i,H_j^\pm,H_k^\pm,\tilde{\nu}_l} \frac{1}{8} C^R_{\tilde{s}u_i H_j^\pm} C^L_{\tilde{u}_i b H_k^\pm} \times \left(C^L_{\tilde{\mu}^- H_k^\pm \nu_l} C^R_{\tilde{\nu}_l H_j^\pm \mu^+} + C^R_{\tilde{\mu}^- H_k^\pm \nu_l} C^L_{\tilde{\nu}_l H_j^\pm \mu^+}\right) \times G_4\left(x_{u_i}, x_{H_j^\pm}, x_{H_k^\pm}, x_{\nu_l}\right),$$

$$C^{(10)}_{10,NP}(\mu_{\rm EW}) = \sum_{u_i,H_j^\pm,H_k^\pm,\tilde{\nu}_l} \frac{1}{8} C^R_{\tilde{s}u_i H_j^\pm} C^L_{\tilde{u}_i b H_k^\pm} \times \left(C^L_{\tilde{\mu}^- H_k^\pm \nu_l} C^R_{\tilde{\nu}_l H_j^\pm \mu^+} - C^R_{\tilde{\mu}^- H_k^\pm \nu_l} C^L_{\tilde{\nu}_l H_j^\pm \mu^+}\right) \times G_4\left(x_{u_i}, x_{H_j^\pm}, x_{H_k^\pm}, x_{\nu_l}\right), \quad \text{(C10)}$$

$$C^{(11)}_{S,NP}(\mu_{\rm EW}) = -\sum_{u_i,H_j^\pm,\nu_l} \frac{1}{2} C^R_{\tilde{s}u_i H_j^\pm} C^R_{\tilde{u}_i b W^\pm} \times C^R_{\tilde{\mu}^- W^\pm \nu_l} C^L_{\tilde{\nu}_l H_j^\pm \mu^+} \times G_4\left(x_{u_i}, x_{H_j^\pm}, x_W, x_{\nu_l}\right),$$

$$C^{(11)}_{P,NP}(\mu_{\rm EW}) = -\sum_{u_i,H_j^\pm,\nu_l} \frac{1}{2} C^R_{\tilde{s}u_i H_j^\pm} C^R_{\tilde{u}_i b W^\pm} C^R_{\tilde{\mu}^- W^\pm \nu_l} \times C^L_{\tilde{\nu}_l H_j^\pm \mu^+} G_4\left(x_{u_i}, x_{H_j^\pm}, x_W, x_{\nu_l}\right). \quad \text{(C11)}$$

$$C^{WW}_{9,NP}(\mu_{\rm EW}) = \sum_{\chi_i^+,\chi_j^0,V} \frac{\left(C^R_{\mu^- V\mu^+} + C^L_{\mu^- V\mu^+}\right) g_s^2}{128\pi^4 s_W^2} \times \frac{m_b^2}{m_b^2 - m_V^2} \times \left\{\left[\left(|C^L_{W^-\tilde{\chi}_j^0\chi_i^+}|^2 + |C^R_{W^-\tilde{\chi}_j^0\chi_i^+}|^2\right) P\left(\frac{1}{8}, \frac{1}{4}, \frac{-1}{48}, \frac{-1}{144}, 1, x_t\right)\right.\right.$$

$$
\begin{aligned}
&+\left(|C^{L}_{W^-\bar{\chi}^0_j\chi_i^+}|^2-|C^{R}_{W^-\bar{\chi}^0_j\chi_i^+}|^2\right)\\
&\times\frac{\partial^1\rho_{1,1}}{\partial x_1}(x_W,x_t)\\
&+\left(C^{R}_{W^-\bar{\chi}^0_j\chi_i^+}C^{L*}_{W^-\bar{\chi}^0_j\chi_i^+}\right.\\
&\times+\left.C^{L}_{W^-\bar{\chi}^0_j\chi_i^+}C^{R*}_{W^-\bar{\chi}^0_j\chi_i^+}\right)\\
&\times P\left(\frac{1}{16},\frac{1}{4},\frac{-1}{16},\frac{1}{144},1,x_t\right)\\
&+\frac{1}{8}\left(C^{L}_{W^-\bar{\chi}^0_j\chi_i^+}C^{R*}_{W^-\bar{\chi}^0_j\chi_i^+}n-C^{R}_{W^-\bar{\chi}^0_j\chi_i^+}\right.\\
&\left.\times C^{L*}_{W^-\bar{\chi}^0_j\chi_i^+}\right)\frac{\partial^2\rho_{2,1}}{\partial x_1^2}(x_W,x_t)\Bigg]C_{VW^-W^-}\\
&+\Bigg[\left(|C^{L}_{W^-\bar{\chi}^0_j\chi_i^+}|^2+|C^{R}_{W^-\bar{\chi}^0_j\chi_i^+}|^2\right)\\
&\times P\left(\frac{1}{144},\frac{-1}{12},\frac{-29}{72},\frac{-11}{12},1,x_t\right)\\
&+\left(C^{R}_{W^-\bar{\chi}^0_j\chi_i^+}C^{L*}_{W^-\bar{\chi}^0_j\chi_i^+}\right.\\
&+\left.C^{L}_{W^-\bar{\chi}^0_j\chi_i^+}C^{R*}_{W^-\bar{\chi}^0_j\chi_i^+}\right)\\
&\times P\left(\frac{-1}{144},\frac{1}{12},\frac{-5}{24},\frac{-1}{12},1,x_t\right)\Bigg]C_{\bar{t}Vt}\\
&+\Bigg[\left(|C^{L}_{W^-\bar{\chi}^0_j\chi_i^+}|^2+|C^{R}_{W^-\bar{\chi}^0_j\chi_i^+}|^2\right)\\
&\times P\left(\frac{3}{16},\frac{3}{16},0,0,1,x_t\right)\\
&+\frac{1}{16}\left(C^{L}_{W^-\bar{\chi}^0_j\chi_i^+}\right.\\
&\times\quad\left.C^{R*}_{W^-\bar{\chi}^0_j\chi_i^+}-C^{R}_{W^-\bar{\chi}^0_j\chi_i^+}C^{L*}_{W^-\bar{\chi}^0_j\chi_i^+}\right)\\
&\times\frac{\partial^2\rho_{2,1}}{\partial x_1^2}(x_W,x_t)\Bigg]\\
&\times\left(C_{\bar{\chi}^0_jV\chi^0_j}+C_{\bar{\chi}^+_iV\chi^+_i}\right)\Big\},
\end{aligned}
\tag{C12}
$$

$$
\begin{aligned}
C^{WW}_{10,NP}(\mu_{\rm EW})=&\sum_{\chi_i^+,\chi_j^0,V}\frac{\left(C^{R}_{\mu^-V\mu^+}-C^{L}_{\mu^-V\mu^+}\right)g_s^2}{128\pi^4s_W^2}\\
&\times\frac{m_b^2}{m_b^2-m_V^2}\\
&\times\Bigg\{\Bigg[\left(|C^{L}_{W^-\bar{\chi}^0_j\chi_i^+}|^2+|C^{R}_{W^-\bar{\chi}^0_j\chi_i^+}|^2\right)\\
&\times P\left(\frac{1}{8},\frac{1}{4},\frac{-1}{48},\frac{-1}{144},1,x_t\right)\\
&\times+\left(|C^{L}_{W^-\bar{\chi}^0_j\chi_i^+}|^2\right.\\
&\left.-|C^{R}_{W^-\bar{\chi}^0_j\chi_i^+}|^2\right)\frac{\partial^1\rho_{1,1}}{\partial x_1}(x_W,x_t)\\
&+\left(C^{R}_{W^-\bar{\chi}^0_j\chi_i^+}C^{L*}_{W^-\bar{\chi}^0_j\chi_i^+}+C^{L}_{W^-\bar{\chi}^0_j\chi_i^+}\right.\\
&\left.\times C^{R*}_{W^-\bar{\chi}^0_j\chi_i^+}\right)P\left(\frac{1}{16},\frac{1}{4},\frac{-1}{16},\frac{1}{144},1,x_t\right)\\
&+\frac{1}{8}\left(C^{L}_{W^-\bar{\chi}^0_j\chi_i^+}C^{R*}_{W^-\bar{\chi}^0_j\chi_i^+}-C^{R}_{W^-\bar{\chi}^0_j\chi_i^+}\right.\\
&\left.\times C^{L*}_{W^-\bar{\chi}^0_j\chi_i^+}\right)\frac{\partial^2\rho_{2,1}}{\partial x_1^2}(x_W,x_t)\Bigg]C_{VW^-W^-}\\
&+\Bigg[\left(|C^{L}_{W^-\bar{\chi}^0_j\chi_i^+}|^2+|C^{R}_{W^-\bar{\chi}^0_j\chi_i^+}|^2\right)\\
&\times P\left(\frac{1}{144},\frac{-1}{12},\frac{-29}{72},\frac{-11}{12},1,x_t\right)\\
&+\left(C^{R}_{W^-\bar{\chi}^0_j\chi_i^+}C^{L*}_{W^-\bar{\chi}^0_j\chi_i^+}\right.\\
&\left.+C^{L}_{W^-\bar{\chi}^0_j\chi_i^+}C^{R*}_{W^-\bar{\chi}^0_j\chi_i^+}\right)\\
&\times P\left(\frac{-1}{144},\frac{1}{12},\frac{-5}{24},\frac{-1}{12},1,x_t\right)\Bigg]C_{\bar{t}Vt}\\
&+\Bigg[\left(|C^{L}_{W^-\bar{\chi}^0_j\chi_i^+}|^2+|C^{R}_{W^-\bar{\chi}^0_j\chi_i^+}|^2\right)\\
&\times P\left(\frac{3}{16},\frac{3}{16},0,0,1,x_t\right)\\
&+\frac{1}{16}\left(C^{L}_{W^-\bar{\chi}^0_j\chi_i^+}\right.\\
&\times\left.C^{R*}_{W^-\bar{\chi}^0_j\chi_i^+}-C^{R}_{W^-\bar{\chi}^0_j\chi_i^+}C^{L*}_{W^-\bar{\chi}^0_j\chi_i^+}\right)\\
&\times\frac{\partial^2\rho_{2,1}}{\partial x_1^2}(x_W,x_t)\Bigg]\\
&\times\left(C_{\bar{\chi}^0_jV\chi^0_j}+C_{\bar{\chi}^+_iV\chi^+_i}\right)\Big\},
\end{aligned}
\tag{C13}
$$

where V denotes photon γ, Z boson, Z' boson. And $C_{\bar{t}Vt}$, $C_{\bar{\chi}^0_jV\chi^0_j}$, $C_{\bar{\chi}^+_iV\chi^+_i}$ denote the vector parts of the corresponding interaction vertex. The concrete expressions for $G_k(k=1,\ldots,4)$ can be given as:

$$
\begin{aligned}
G_1(x_1,x_2,x_3)=&\frac{-1}{m_W^2}\left[\frac{x_1\ln x_1}{(x_2-x_1)(x_3-x_1)}\right.\\
&+\frac{x_2\ln x_2}{(x_1-x_2)(x_3-x_2)}\\
&\left.+\frac{x_3\ln x_3}{(x_1-x_3)(x_2-x_3)}\right],\\
G_2(x_1,x_2,x_3)=&-\frac{x_1^2\ln x_1}{(x_2-x_1)(x_3-x_1)}\\
&-\frac{x_2^2\ln x_2}{(x_1-x_2)(x_3-x_2)}\\
&-\frac{x_3^2\ln x_3}{(x_1-x_3)(x_2-x_3)},
\end{aligned}
$$

$$G_3(x_1,x_2,x_3,x_4)=\frac{1}{m_W^4}\left[\frac{x_1\ln x_1}{(x_2-x_1)(x_3-x_1)(x_4-x_1)}\right.$$
$$+\frac{x_2\ln x_2}{(x_1-x_2)(x_3-x_2)(x_4-x_2)}$$
$$+\frac{x_3\ln x_3}{(x_1-x_3)(x_2-x_3)(x_4-x_3)}$$
$$\left.\times\frac{x_4\ln x_4}{(x_1-x_4)(x_2-x_4)(x_3-x_4)}\right],$$
$$G_4(x_1,x_2,x_3,x_4)=\frac{1}{m_W^2}\left[\frac{x_1^2\ln x_1}{(x_2-x_1)(x_3-x_1)(x_4-x_1)}\right.$$
$$+\frac{x_2^2\ln x_2}{(x_1-x_2)(x_3-x_2)(x_4-x_2)}$$
$$+\frac{x_3^2\ln x_3}{(x_1-x_3)(x_2-x_3)(x_4-x_3)}$$
$$\left.\times\frac{x_4^2\ln x_4}{(x_1-x_4)(x_2-x_4)(x_3-x_4)}\right]. \quad \text{(C14)}$$

References

1. C. Partignani et al. [PDG Collaboration], Chin. Phys. C **40**, 100001 (2016) **(and 2017 update)**
2. J.P. Lees et al., BaBar Collaboration. Phys. Rev. Lett. **109**, 191801 (2012). arXiv:1207.2690 [hep-ex]
3. J.P. Lees et al., BaBar Collaboration. Phys. Rev. D **86**, 052012 (2012). arXiv:1207.2520 [hep-ex]
4. T. Saito et al., Belle Collaboration. Phys. Rev. D **91**, 052004 (2015). arXiv:1411.7198 [hep-ex]
5. K. Adel, Y.-P. Yao, Phys. Rev. D **49**, 4945 (1994)
6. A. Ali, C. Greub, Phys. Lett. B **361**, 146 (1995)
7. C. Greub, T. Hurth, D. Wyler, Phys. Rev. D **54**, 3350 (1996)
8. K. Chetyrkin, M. Misiak, M. Munz, Phys. Lett. B **400**, 206 (1997)
9. M. Misiak et al., Phys. Rev. Lett. **98**, 022002 (2007)
10. M. Misiak, M. Steinhauser, Nucl. Phys. B **764**, 62 (2007)
11. A.J. Buras, J. Girrbach, G. Isidori, Eur. Phys. J. C **72**, 2172 (2012)
12. M. Misiak, Phys. Rev. Lett. **114**, 221801 (2015). arXiv:1503.01789 [hep-ph]
13. M. Czakon, P. Fiedler, T. Huber, M. Misiak, T. Schutzmeier, M. Steinhauser, JHEP **1504**, 168 (2015). arXiv:1503.01791 [hep-ph]
14. P.H. Chankowski, L. Slawianowska, Phys. Rev. D **63**, 054012 (2001). arXiv:hep-ph/0008046
15. C. Bobeth, T. Ewerth, F. Kruger, J. Urban, Phys. Rev. D **66**, 074021 (2002). arXiv:hep-ph/0204225
16. S. Baek, Phys. Lett. B **595**, 461 (2004). arXiv:hep-ph/0406007
17. M. Beneke, X.Q. Li, L. Vernazza, Eur. Phys. J. C **61**, 429 (2009). arXiv:0901.4841 [hep-ph]
18. D. Feldman, Z. Liu, P. Nath, Phys. Rev. D **81**, 117701 (2010). arXiv:1003.0437 [hep-ph]
19. R.M. Wang, Y.G. Xu, Y.L. Wang, Y.D. Yang, Phys. Rev. D **85**, 094004 (2012). arXiv:1112.3174 [hep-ph]
20. P. Colangelo, F. Giannuzzi, S. Nicotri, F. Zuo, Phys. Rev. D **88**, 115011 (2013). arXiv:1308.0489 [hep-ph]
21. S.S. AbdusSalam, L. Velasco-Sevilla, arXiv:1707.04752 [hep-ph]
22. M. Ciuchini, G. Degrassi, P. Gambino, G.F. Giudice, Nucl. Phys. B **527**, 21 (1998)
23. P. Ciafaloni, A. Romanino, A. Strumia, Nucl. Phys. B **524**, 361 (1998)
24. F. Borzumati, C. Greub, Phys. Rev. D **58**, 074004 (1998)
25. S. Bertolini, F. Borzumati, A. Masiero, G. Ridolfi, Nucl. Phys. B **353**, 591 (1991)
26. R. Barbieri, G.F. Giudice, Phys. Lett. B **309**, 86 (1993)
27. F. Borzumati, C. Greub, T. Hurth, D. Wyler, Phys. Rev. D **62**, 075005 (2000)
28. S. Prelovsek, D. Wyler, Phys. Lett. B **500**, 304 (2001)
29. M. Causse, J. Orloff, Eur. Phys. J. C **23**, 749 (2002)
30. H.-B. Zhang, G.-H. Luo, T.-F. Feng, S.-M. Zhao, T.-J. Gao, K.-S. Sun, Mod. Phys. Lett. A **29**, 1450196 (2014). arXiv:1409.6837 [hep-ph]
31. T.-F. Feng, Y.-L. Yan, H.-B. Zhang, S.-M. Zhao, Phys. Rev. D **92**, 055024 (2015)
32. M. Ciuchini, G. Degrassi, P. Gambino, G.F. Giudice, Nucl. Phys. B **534**, 3 (1998)
33. X.G. He, T.D. Nguyen, R.R. Volkas, Phys. Rev. D **38**, 814 (1988)
34. W. Skiba, J. Kalinowski, Nucl. Phys. B **404**, 3 (1993)
35. S.R. Choudhury, N. Gaur, Phys. Lett. B **451**, 86 (1999). arXiv:hep-ph/9810307
36. C.S. Huang, W. Liao, Q.S. Yan, S.H. Zhu, Phys. Rev. D **63**, 114021 (2001) [Erratum, ibid. **64**, 059902 (2001)]. arXiv:hep-ph/0006250
37. T.-F. Feng, Y.-L. Yan, H.-B. Zhang, S.-M. Zhao, Int. J. Mod. Phys. A **31**, 1650092 (2016). arXiv:1603.07578 [hep-ph]
38. T.-F. Feng, J.-L. Yang, H.-B. Zhang, S.-M. Zhao, R.-F. Zhu, Phys. Rev. D **94**, 115034 (2016). arXiv:1612.02094 [hep-ph]
39. W.N. Cottingham, H. Mehrban, I.B. Whittingham, Phys. Rev. D **60**, 114029 (1999)
40. G. Barenboim, M. Raidal, Phys. Lett. B **457**, 109 (1999)
41. J.L. Hewett, D. Wells, Phys. Rev. D **55**, 5549 (1997)
42. A. Masiero, L. Silvestrini, B Physics and CP Violation, Honolulu, p. 172 (1997). arXiv:hep-ph/9709244
43. A. Masiero, L. Silvestrini, Highlights of Subnuclear Physics, Erice, p. 404, (1997). arXiv:hep-ph/9711401
44. M. Ambroso, B.A. Ovrut, Int. J. Mod. Phys. A **26**, 1569–1627 (2010)
45. P.F. Perez, S. Spinner, Phys. Rev. D **83**, 035004 (2011)
46. W. Abdallah, A. Hammad, S. Khalil, S. Moretti, Phys. Rev. D **95**, 055019 (2017). arXiv:1608.07500 [hep-ph]
47. A. Elsayed, S. Khalil, S. Moretti, Phys. Lett. B **715**, 208 (2012). arXiv:1106.2130 [hep-ph]
48. G. Brooijmans et al., arXiv:1203.1488 [hep-ph]
49. L. Basso, F. Staub, Phys. Rev. D **87**, 015011 (2013). arXiv:1210.7946 [hep-ph]
50. L. Basso, Comput. Phys. Commun. **184**, 698 (2013). arXiv:1206.4563 [hep-ph]
51. A. Elsayed, S. Khalil, S. Moretti, A. Moursy, Phys. Rev. D **87**, 053010 (2013). arXiv:1211.0644 [hep-ph]
52. S. Khalil, S. Moretti, Rep. Prog. Phys. **80**, 036201 (2017). arXiv:1503.08162 [hep-ph]
53. A. Das, S. Oda, N. Okada, D. s. Takahashi, Phys. Rev. D **93**, 115038, (2016), arXiv:1605.01157
54. A. Das, T. Nomura, H. Okada, S. Roy, Phys. Rev. D **96**, 075001 (2017). arXiv:1704.02078
55. A. Das, N. Okada, D. Raut, Phys. Rev. D **97**, 115023 (2018). arXiv:1710.03377
56. C.S. Aulakh, A. Melfo, A. Rasin, G. Senjanovic, Phys. Lett. B **459**, 557 (1999). arXiv:hep-ph/9902409
57. S. Khalil, A. Masiero, Phys. Lett. B **665**, 374 (2008). arXiv:0710.3525 [hep-ph]
58. T.R. Dulaney, P. Fileviez Perez, M.B. Wise, Phys. Rev. D **83**, 023520 (2011). arXiv:1005.0617 [hep-ph]
59. V. Barger, P. Fileviez Perez, S. Spinner, Phys. Rev. Lett. **102**, 181802 (2009). arXiv:0812.3661 [hep-ph]
60. J. Pelto, I. Vilja, H. Virtanen, Phys. Rev. D **83**, 055001 (2011). arXiv:1012.3288 [hep-ph]
61. K.S. Babu, Y. Meng, Z. Tavartkiladze, Phys. Lett. B **681**, 37 (2009). arXiv:0901.1044 [hep-ph]

62. S. Khalil, H. Okada, Phys. Rev. D **79**, 083510 (2009). arXiv:0810.4573 [hep-ph]
63. L. Basso, B. OLeary, W. Porod, F. Staub, JHEP **1209**, 054 (2012). arXiv:1207.0507 [hep-ph]
64. L. Delle Rose, S. Khalil, S.J.D. King, C. Marzo, S. Moretti, C.S. Un, Phys. Rev. D **96**, 055004 (2017). arXiv:1702.01808 [hep-ph]
65. L. Delle Rose, S. Khalil, S.J.D. King, S. Kulkarni, C. Marzo, S. Moretti, C.S. Un, arXiv:1712.05232 [hep-ph]
66. B. OLeary, W. Porod, F. Staub, JHEP **1205**, 042 (2012). arXiv:1112.4600 [hep-ph]
67. L. Basso, Adv. High Energy Phys. **2015**, 980687 (2015). arXiv:1504.05328 [hep-ph]
68. S. Khalil, C.S. Un, Phys. Lett. B **763**, 164 (2016). arXiv:1509.05391 [hep-ph]
69. A. Hammad, S. Khalil, S. Moretti, Phys. Rev. D **93**, 115035 (2016). arXiv:1601.07934 [hep-ph]
70. F. Staub, arXiv:0806.0538
71. F. Staub, Comput. Phys. Commun. **181**, 1077–1086 (2010). arXiv:0909.2863
72. F. Staub, Comput. Phys. Commun. **182**, 808–833 (2011). arXiv:1002.0840
73. F. Staub, Comput. Phys. Commun. **184**, 1792–1809 (2013). arXiv:1207.0906
74. F. Staub, Comput. Phys. Commun. **185**, 1773–1790 (2014). arXiv:1309.7223
75. B. Holdom, Phys. Lett. B **166**, 196 (1986)
76. T. Matsuoka, D. Suematsu, Prog. Theor. Phys. **76**, 901 (1986)
77. F. del Aguila, G.D. Coughlan, M. Quiros, Nucl. Phys. B **307**, 633 (1988)
78. F. del Aguila, J.A. Gonzalez, M. Quiros, Nucl. Phys. B **307**, 571 (1988)
79. F. del Aguila, G.D. Coughlan, M. Quiros, Nucl. Phys. B **312**, 751 (1989)
80. R. Foot, X.G. He, Phys. Lett. B **267**, 509 (1991)
81. K.S. Babu, C.F. Kolda, J. March-Russell, Phys. Rev. D **57**, 6788 (1998). arXiv:hep-ph/9710441
82. R. Fonseca, M. Malinsky, W. Porod, F. Staub, Nucl. Phys. B **854**, 28–53 (2012). arXiv:1107.2670 [hep-ph]
83. P.H. Chankowski, S. Pokorski, J. Wagner, Eur. Phys. J. C **47**, 187–205 (2006)
84. M. Carena, J.R. Espinosaos, C.E.M. Wagner, M. Quir, Phys. Lett. B **355**, 209 (1995)
85. M. Carena, M. Quiros, C.E.M. Wagner, Nucl. Phys. B **461**, 407 (1996)
86. M. Carena, S. Gori, N.R. Shah, C.E.M. Wagner, JHEP **03**, 014 (2012)
87. R. Grigjanis, P.J. ODonnell, M. Sutherland, H. Navelet. Phys. Rep. **22**, 93 (1993)
88. G. Buchalla, A.J. Buras, M.E. Lautenbacher, Rev. Mod. Phys. **68**, 1125 (1996)
89. W. Altmannshofer, P. Ball, A. Bharucha, A.J. Buras, D.M. Straub, M. Wick, JHEP **0901**, 019 (2009). arXiv:0811.1214 [hep-ph]
90. L. Lin, T.-F. Feng, F. Sun, Mod. Phys. Lett. A **24**, 2181–2186 (2009)
91. X.-Y. Yang, T.-F. Feng, JHEP **1005**, 059 (2010)
92. P. Goertz, T. Pfoh, Phys. Rev. D **84**, 095016 (2011)
93. A.J. Buras, L. Merlo, E. Stamou, JHEP **1108**, 124 (2011)
94. F. Goertz, T. Pfoh, Phys. Rev. D **84**, 095016 (2011)
95. P. Gambino, M. Misiak, Nucl. Phys. B **611**, 338 (2001)
96. M. Czakon, U. Haisch, M. Misiak, JHEP **0703**, 008 (2007)
97. A.J. Buras, M. Misiak, M. Müunz, S. Pokorski, Nucl. Phys. B **424**, 374 (1994)
98. T.-J. Gao, T.-F. Feng, J.-B. Chen, Mod. Phys. Lett. A **7**, 1250011 (2012)
99. P. Gambino, M. Gorbahn, U. Haisch, Nucl. Phys. B **673**, 238 (2003)
100. ATLAS Collab., ATLAS-CONF-2016-045, 38th International Conference on High Energy Physics, Chicago, IL, USA, 03–10 Aug 2016
101. G. Cacciapaglia, C. Csaki, G. Marandella, A. Strumia, Phys. Rev. D **74**, 033011 (2006). arXiv:hep-ph/0604111
102. M. Carena, A. Daleo, B.A. Dobrescu, T.M.P. Tait, Phys. Rev. D **70**, 093009 (2004). arXiv:hep-ph/0408098
103. ATLAS Collab., Phys. Rev. D **87**, 012008 (2013)
104. CMS Collab., JHEP **1210**, 018 (2012)
105. C.S. Un, O. Ozdal, Phys. Rev. D **93**, 055024 (2016). arXiv:1601.02494 [hep-ph]
106. F. Domingo, U. Ellwanger, JHEP **0712**, 090 (2007)